# Supplemental materials for:

# Intestinal microbiota metabolism of *L*-carnitine, a nutrient in red meat, promotes atherosclerosis

Robert A. Koeth[1,2], Zeneng Wang[1,2], Bruce S. Levison[1,2], Jennifer A. Buffa[1,2], Elin Org[3], Brendan T. Sheehy[1], Earl B. Britt[1,2], Xiaoming Fu[1,2], Yuping Wu[4], Lin Li[1,2], Jonathan D. Smith[1,2,5], Joseph A. DiDonato[1,2], Jun Chen[6], Hongzhe Li[6], Gary D. Wu[7], James D. Lewis [6,8], Manya Warrier[9], J. Mark Brown[9], Ronald M. Krauss[10], W. H. Wilson Tang[1,2,5], Frederic D. Bushman[5], Aldons J. Lusis[3], and Stanley L. Hazen[1,2, 5]

[1]Department of Cellular & Molecular Medicine, [2]Center for Cardiovascular Diagnostics and Prevention, and [5]Department of Cardiovascular Medicine, Cleveland Clinic, Cleveland, Ohio 44195, USA.
[3]Department of Medicine/Division of Cardiology, David Geffen School of Medicine, University of California, Los Angeles 90095, USA.
[4]Department of Mathematics, Cleveland State University, Cleveland, Ohio 44115, USA.
[6]Department of Microbiology, Center for Clinical Epidemiology and Biostatistics, [7]Division of Gastroenterology, and [8] Department of Medicine, Perelman School of Medicine at the University of Pennsylvania, Philadelphia, PA 19104, USA.
[9]Department of Pathology, Section on Lipid Sciences, Wake Forest School of Medicine, Winston-Salem, NC 27157, USA.
[10] Children's Hospital Oakland Research Institute, Oakland, CA 94609, USA.

Address for Correspondence:
Stanley L. Hazen, MD PhD
Department of Cellular & Molecular Medicine, Cleveland Clinic
9500 Euclid Avenue, NC-10
Cleveland, OH 44195
Phone: (216) 445-9763
Fax: (216) 444-9404
E-mail: hazens@ccf.org

**Supplementary Table 1**

Learning cohort

| Analytes *m/z* | Retention Time (min) | Peak Area | | | Hazard ratio (95% CI) | *P* for trend |
|---|---|---|---|---|---|---|
| | | Control | Case | adjusted Log(*P*) | | |
| 162 | 5.10 | 7.95E+08 | 8.40E+08 | 1.13 | 4.73 (1.50-14.9) | < 0.01 |

Validation cohort

| Analytes *m/z* | Retention Time (min) | Peak Area | | | Hazard ratio (95% CI) | *P* for trend |
|---|---|---|---|---|---|---|
| | | Control | Case | adjusted Log(*P*) | | |
| 162 | 5.10 | 7.89E+08 | 7.96E+08 | 0.07 | 1.41 (0.29-6.96) | 0.67 |

Learning + Validation cohort

| Analytes *m/z* | Retention Time (min) | Peak Area | | | Hazard ratio (95% CI) | *P* for trend |
|---|---|---|---|---|---|---|
| | | Control | Case | adjusted Log(*P*) | | |
| 162 | 5.10 | 7.91E+08 | 8.21E+08 | 0.82 | 2.63 (1.03-6.75) | 0.04 |

**Characteristics of analyte *m/z* = 162 determined in LC/MS positive ion mode from plasma samples used in Validation and Learning cohorts (*n* = 150) of metabolomics study from Wang et. al., *Nature*, 2011.** Plasma samples used in the metabolomics study described in Wang et al [1] were from GeneBank, a large clinical repository of patients undergoing elective diagnostic cardiac evaluation. The original study utilized a Learning cohort of 50 cases (randomly selected GeneBank subjects who experienced death, non-fatal MI, or stroke in the ensuing 3 year follow up period) and 50 age and gender matched controls (subjects with no ensuing history of death, non-fatal MI or stroke in the 3 year period after enrollment). Peaks within LC chromatograms from the metabolomics analyses that exceeded a signal to noise ratio of greater than 5 were integrated. Bonferroni adjusted two sided T-tests were calculated and adjusted – logP value > 1.3 were considered significant. An odds ratio (OR) between the highest and lowest quartile was calculated for each unknown analyte. Only analytes with 95% confidence intervals not crossing unity were considered significant. Additionally, Cochran-Armitage trend tests across the quartiles were performed with $P < 0.05$ being considered significant. A similar analysis was performed in a non-overlapping Validation cohort consisting of 25 additional cases and controls from GeneBank. In both Learning and Validation cohorts only 18 plasma analytes met this strict set of validation criterion, and an analyte with *m/z* =162 (same as carnitine) was not among them [1]. Results for an analyte with *m/z* = 162 and retention time similar to that of authentic L-carnitine in the Learning and Validation cohorts are shown. In a new hypothesis-generated analysis that did not adjust for multiple sampling (since only an analyte was being examined) and that used the combined data set (Learning + Validation cohorts, *n* = 75 cases and *n* = 75 age-gender matched controls), the plasma analyte with *m/z* = 162 and retention time identical to carnitine was significantly associated with cardiovascular risks (bottom table, $P = 0.04$). These results suggested that plasma levels of an analyte with *m/z* = 162, perhaps L-carnitine, may be associated with cardiovascular risks. Further details regarding the analyses of the original metabolomics data reported in ref. 1 can be found in **Supplementary Methods**.

**Supplementary Table 2**

| Patient Characteristics | Whole cohort | Carnitine Quartiles Q1 | Q2 | Q3 | Q4 | *P* |
|---|---|---|---|---|---|---|
| | | < 31.7 µM | 31.7 - 37.8 µM | 37.9 - 45.2 µM | > 45.2 µM | |
| | (*n* = 2595) | (*n* = 649) | (*n* = 647) | (*n* = 649) | (*n* = 650) | |
| Age (years) | 62 (54-71) | 63 (54-72) | 62(54-71) | 63(54-71) | 61 (53-71) | < 0.01 |
| Male (%) | 70 | 54 | 69 | 76 | 80 | < 0.01 |
| Smoking (%) | 69 | 61 | 67 | 71 | 77 | < 0.01 |
| Diabetes mellitus (%) | 28 | 27 | 26 | 27 | 31 | 0.20 |
| Hypertension (%) | 72 | 69 | 72 | 73 | 75 | 0.06 |
| Hyperlipidemia (%) | 85 | 81 | 86 | 87 | 88 | < 0.01 |
| Prior CAD (%) | 74 | 65 | 73 | 75 | 83 | < 0.01 |
| CAD (%) | 78 | 70 | 76 | 80 | 85 | < 0.01 |
| PAD (%) | 22 | 22 | 19 | 21 | 26 | 0.01 |
| CVD (%) | 80 | 71 | 78 | 82 | 88 | < 0.01 |
| BMI ($kg/m^2$) | 29 (25-33) | 28 (24-31) | 29 (2-32) | 29 (25-32) | 29 (26-34) | < 0.01 |
| LDL cholesterol ($mg\ dl^{-1}$) | 96 (78-117) | 94 (74-111) | 100 (80-122) | 97 (80-117) | 96 (77-117) | < 0.01 |
| HDL cholesterol ($mg\ dl^{-1}$) | 34( 28-41) | 35 (30-43) | 34 (28-41) | 32 (27-39) | 32 (27-38) | < 0.01 |
| Total cholesterol ($mg\ dl^{-1}$) | 160 (139-188) | 159 (138-184) | 164 (140-194) | 160 (139-188) | 161 (139-188) | < 0.01 |
| Triglycerides ($mg\ dl^{-1}$) | 117 (85-167) | 103 (76-148) | 110 (84-159) | 124 (88-170) | 129 (96-192) | < 0.01 |
| hsCRP ($mg\ l^{-1}$) | 2.3 (1.0-5.4) | 2.3 (1.0-5.5) | 2.1 (1.0-5.0) | 2.2 (1.0-5.0) | 2.5 (1.1-6.0) | < 0.01 |
| MPO ($pmol\ l^{-1}$) | 113 (76-230) | 122 (75-267) | 109 (73-205) | 110 (76-215) | 114 (79-234) | < 0.01 |
| eGFR ($ml\ min/1.73/m^2$) | 83 (70-96) | 86 (73-99) | 85 (73-98) | 83 (70-95) | 79 (64-93) | < 0.01 |
| Carnitine (µM) | 38 (32-45) | 28 (25-30) | 35 (33-36) | 41 (39-43) | 51 (48-56) | < 0.01 |
| **Baseline medications (%)** | | | | | | |
| ACE inhibitors | 51 | 45 | 51 | 51 | 57 | < 0.01 |
| Beta-blockers | 67 | 62 | 63 | 68 | 73 | < 0.01 |
| Statin | 63 | 58 | 64 | 65 | 64 | 0.06 |
| Aspirin | 76 | 75 | 77 | 76 | 76 | 0.82 |

**Subject characteristics, demographics, and laboratory values in the whole cohort (*n* = 2595), and across quartiles of plasma carnitine.** Values are expressed in mean ± SD for normally distributed variables, or median (interquartile range) for non-normally distributed variables. The *P* value represents a Kruskal Wallis test for continuous variables and Chi-square test for categorical variables across quartiles of carnitine. Abbreviations: ACE, angiotensin converting enzyme; ATP III, Adult Treatment Panel III guidelines; BMI, body mass index; CAD, coronary artery disease; CVD, cardiovascular disease; cTnI = cardiac Troponin I; HDL, high-density lipoprotein; hsCRP, high-sensitivity C-reactive protein; LDL, low-density lipoprotein; MPO, myeloperoxidase; PAD, peripheral artery disease.

**Supplementary Table 3**

## -Antibiotics

| Plasma Lipids | Chow ($n$ = 9) | 1.3% Carnitine ($n$ = 11) | *P* |
|---|---|---|---|
| Triglyceride (mg $dl^{-1}$) | 110±27 | 118±22 | 0.52 |
| Total Cholesterol (mg $dl^{-1}$) | 347±56 | 384±70 | 0.21 |
| Total Glucose (mg $dl^{-1}$) | 200±49 | 257±76 | 0.07 |
| Insulin (μg $dl^{-1}$) | 0.57± 0.37 | 0.91± 0.96 | 0.33 |

## +Antibiotics

| Plasma Lipids | Chow,+ABS ($n$ = 9) | 1.3% Carnitine,+ABS ($n$ = 10) | *P* |
|---|---|---|---|
| Triglyceride (mg $dl^{-1}$) | 98±22 | 92±19 | 0.52 |
| Total Cholesterol (mg $dl^{-1}$) | 499±113 | 562±67 | 0.25 |
| Total Glucose (mg $dl^{-1}$) | 223±173 | 213±35 | 0.77 |
| Insulin (μg $dl^{-1}$) | 0.46±0.32 | 0.37±0.21 | 0.64 |

**Plasma levels of triglycerides, cholesterol, glucose, and insulin from mice on normal chow vs. carnitine supplemented diet.** C57BL/6J, *Apoe*$^{-/-}$ female mice at time of weaning were placed on the indicated diets until time of sacrifice for aortic root quantification of atherosclerosis (19 weeks of age). Parallel groups of animals were also provided an antibiotics cocktail in drinking water as described under **Supplementary Methods**. Lipid profiles, glucose, and insulin levels shown were determined in plasma isolated at time of organ harvest at conclusion of study. Data shown are mean ± SD for each of the indicated feeding groups. Student t-test comparisons are between chow and carnitine (1.3%) supplemented diets with the noted antibiotic (ABS) treatment status.

**Supplementary Table 4**

## -Antibiotics

| Liver Lipids | Chow ($n$ = 9) | 1.3% Carnitine ($n$ = 11) | *P* |
|---|---|---|---|
| Triglyceride (mg $g^{-1}$ liver) | 29±9.0 | 31±11 | 0.59 |
| Total Cholesterol (mg $g^{-1}$ liver) | 1.6±0.21 | 1.1±0.38 | 0.004 |

## +Antibiotics

| Liver Lipids | Chow,+ABS ($n$ = 9) | 1.3% Carnitine,+ABS ($n$ = 10) | *P* |
|---|---|---|---|
| Triglyceride (mg $g^{-1}$ liver) | 23±7.1 | 16±1.7 | 0.11 |
| Total Cholesterol (mg $g^{-1}$ liver) | 1.7±0.22 | 1.8±0.49 | 0.34 |

**Liver levels of triglycerides and total cholesterol in mice on normal chow versus carnitine supplemented diet.** Liver was harvested from female C57BL/6J, *Apoe*$^{-/-}$ mice on the indicated diets at time of sacrifice for aorta harvest for aortic root quantification (19 weeks of age and 15 weeks on diets). Liver was homogenized and the content of triglycerides and total cholesterol determined as described under **Supplementary Methods**. Data are presented as mean ± SD for each of the indicated groups of mice. A student t-test comparison was performed between chow and carnitine groups on or off a cocktail of oral broad spectrum antibiotics (+ ABS) as described in **Supplementary Methods**. No significant increases in liver lipid levels were noted in the carnitine supplemented mice compared to the respective chow controls.

**Supplementary Table 5**

## TMAO RCT

| Plasma | Chow ($n$ = 21) | 0.12% TMAO ($n$ = 27) | $P$ |
|---|---|---|---|
| **Triglyceride (mg dl$^{-1}$)** | 52.3±11.5 | 45.7±24.6 | 0.05 |
| **Total Cholesterol (mg dl$^{-1}$)** | 251.9±53 | 225.7±119 | 0.07 |
| **Total Glucose (mg dl$^{-1}$)** | 178±36 | 168±21 | 0.28 |
| **HDL Cholesterol (mg dl$^{-1}$)** | 47.3±14 | 44.7±8.3 | 0.46 |

## Carnitine and Choline RCT

| Plasma | Chow ($n$ = 43) | 1.3% Carnitine ($n$ = 27) | $P$ | 1.0% Choline ($n$ = 21) | $P$ |
|---|---|---|---|---|---|
| **Triglyceride (mg dl$^{-1}$)** | 70±27 | 66±13 | 0.48 | 55±28 | 0.02 |
| **Total Cholesterol (mg dl$^{-1}$)** | 280±58 | 308±87 | 0.15 | 275±109 | 0.39 |
| **Total Glucose (mg dl$^{-1}$)** | 187±37 | 170±43 | 0.12 | 151±19 | < 0.01 |
| **HDL Cholesterol (mg dl$^{-1}$)** | 55±20 | 54±17 | 0.52 | 50±20 | 0.52 |

**Plasma levels of triglycerides, cholesterol, and glucose from mice on normal chow, carnitine, choline, and TMAO supplemented diets during the *in vivo* RCT studies.** C57BL/6J, *Apoe*$^{-/-}$ female mice were enrolled in two separate studies to quantify *in vivo* reverse cholesterol transport (RCT) by placement on the indicated diets at time of weaning ("TMAO RCT" study, and "Carnitine and Choline RCT" study). Following 4 weeks of diet, [$^{14}$C]cholesterol loaded macrophages were injected subcutaneously, and *in vivo* RCT quantified as described under **Supplementary Methods**. Lipid profiles and glucose levels shown were determined in plasma isolated at time of organ harvest at conclusion of study (72h post injection of [$^{14}$C]cholesterol loaded macrophages). Data shown are mean ± SD for each of the indicated dietary groups.

**Supplementary Figure 1**

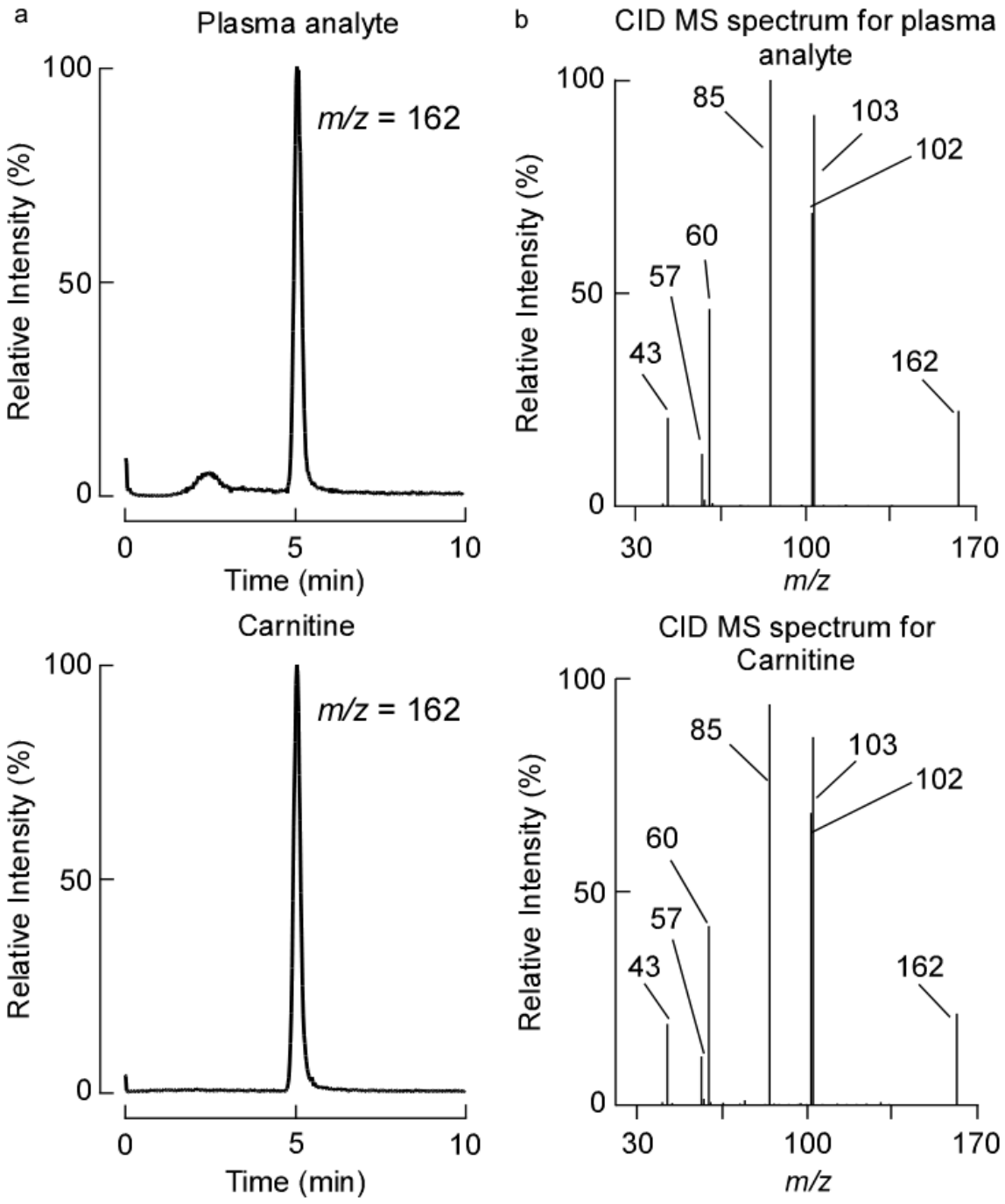


**Mass spectrometry analyses identify unknown plasma analyte at retention time of 5.1 min and *m/z* = 162 as carnitine. a)** Extracted ion chromatograms at *m/z* = 162 from human plasma sample (top), and authentic L-carnitine standard (bottom). Identical retention times under multiple chromatographic conditions during LC/MS analysis were demonstrated for analyte *m/z* =162 and L-carnitine standard. **b)** Collision-induced dissociation (CID) spectra from 5.10 min peak in human plasma and L-carnitine standard. This data demonstrate that the analyte at 5.10 min with *m/z* = 162 from human plasma possesses identical CID mass spectrum and retention time to authenticate synthetic L-carnitine standard.

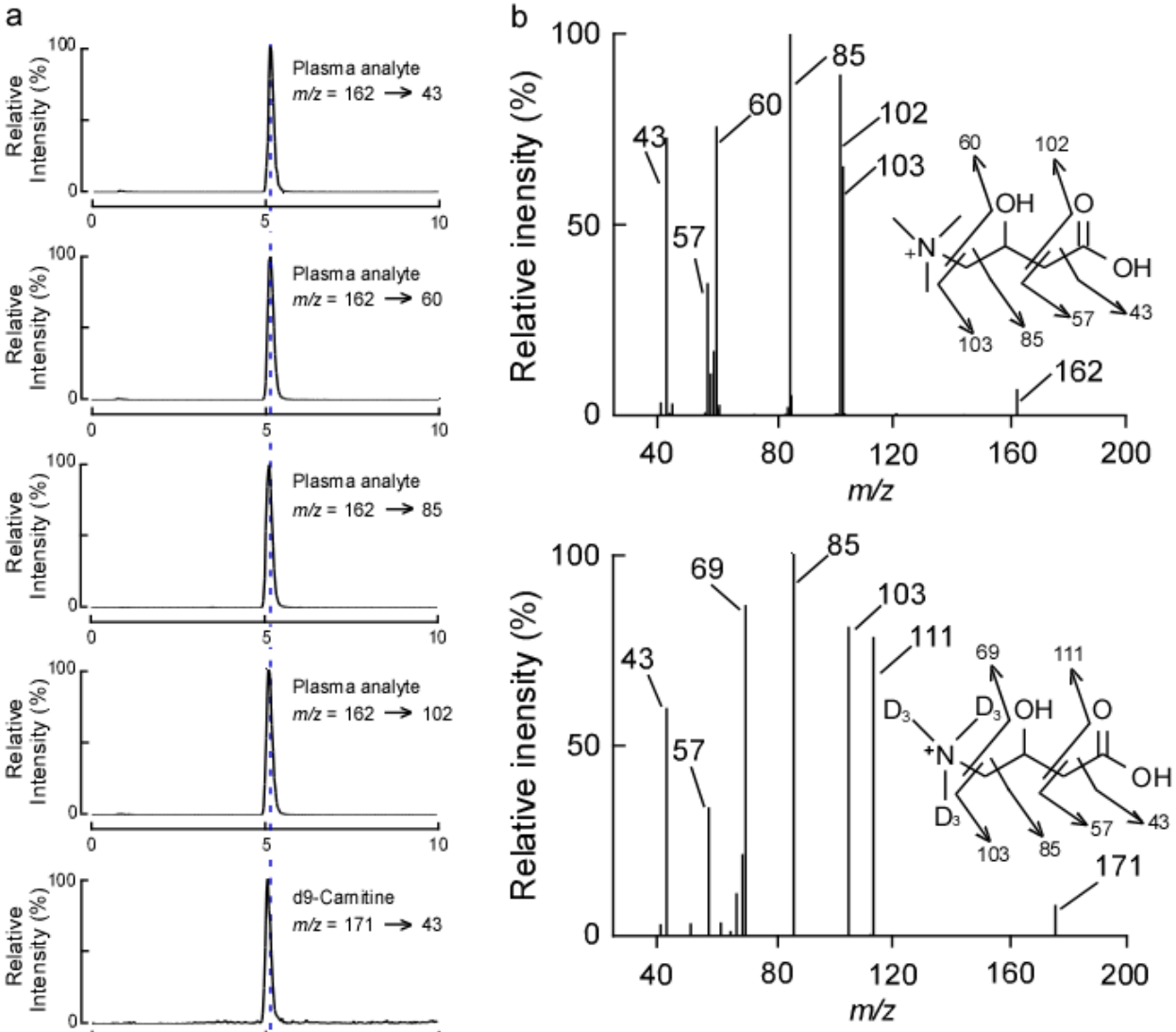


**LC/MS/MS analysis of synthetic heavy isotope standard d9(trimethyl)carnitine spiked into human plasma sample confirms unknown peak at 5.10 min (*m/z* = 162) is carnitine**. **a)** Human plasma was spiked with synthetic d9(trimethyl)-carnitine. The sample was then analyzed by LC/MS/MS using multiple distinct precursor → product ion transitions in multiple reaction monitoring (MRM) mode that are characteristic for L-carnitine and its d9(trimethyl)-isotopologue. Note that multiple characteristic precursor → product transitions demonstrate identical retention times for both the plasma analyte with *m/z* = 162, and synthetic d9(trimethyl)-carnitine standard. **b)** Precursor → product ion transitions were determined from CID spectra of both authentic L-carnitine and synthetic d9(trimethyl)carnitine. Insets: Shown are proposed fragmentation overlay on structure from positive ion electrospray analyses of L-carnitine and d9-carnitine.

**Supplementary Figure 3**

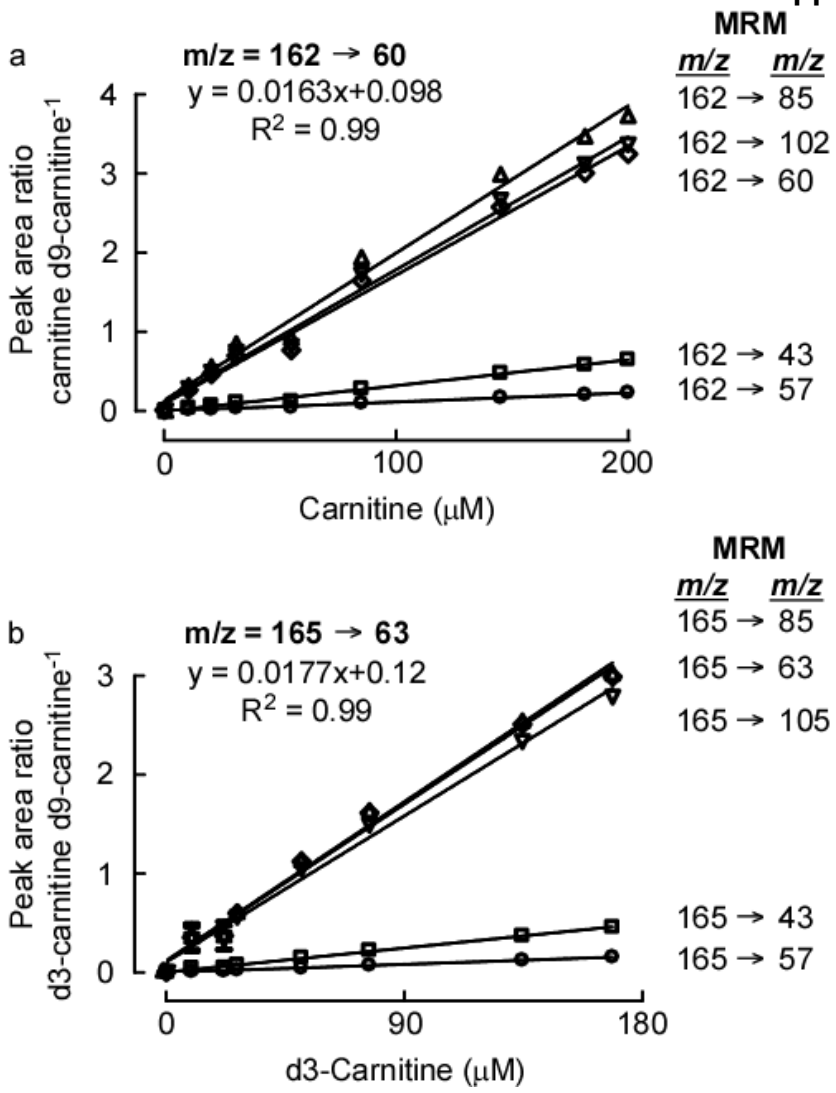


**Standard curves for LC/MS/MS quantification of carnitine and d3-(methyl)-carnitine in plasma matrix.** We used synthetic d9(trimethyl)carnitine as internal standard to quantify d3(methyl)carnitine, and natural abundance carnitine isotopologues in plasma recovered from mice and humans following carnitine challenge. To generate standard curves for each isotopologue in plasma matrix, a fixed amount of d9-(trimethyl)carnitine as an internal standard was added to dialyzed human plasma, and increasing concentrations of L-carnitine (**a**) and synthetic d3-(methyl)carnitine (**b**) were spiked into the samples. Plasma proteins were precipitated with a methanol at 0°C. Aliquots of the supernatant solution were analyzed by LC with on-line tandem mass spectrometry using electrospray ionization in positive ion mode on an AB SCIEX 5000 triple quadrupole mass spectrometer. Unique precursor → product ion transitions were selected for carnitine and its d3- and d9-isotopologues. Areas of peaks from multiple reaction monitoring (MRM) were divided by the peak area from *m/z* transition 171 → 69 from d9-carnitine. Standard curves of peak area ratio versus known concentrations are plotted on the same axis for carnitine (**a**) and d3-carnitine (**b**). For quantification, precursor → product transitions of 162 → 60 and 165 → 63 were typically used to measure carnitine and d3-carnitine, respectively, and if needed, alternative indicated transitions used to confirm results.

**Supplementary Figure 4**

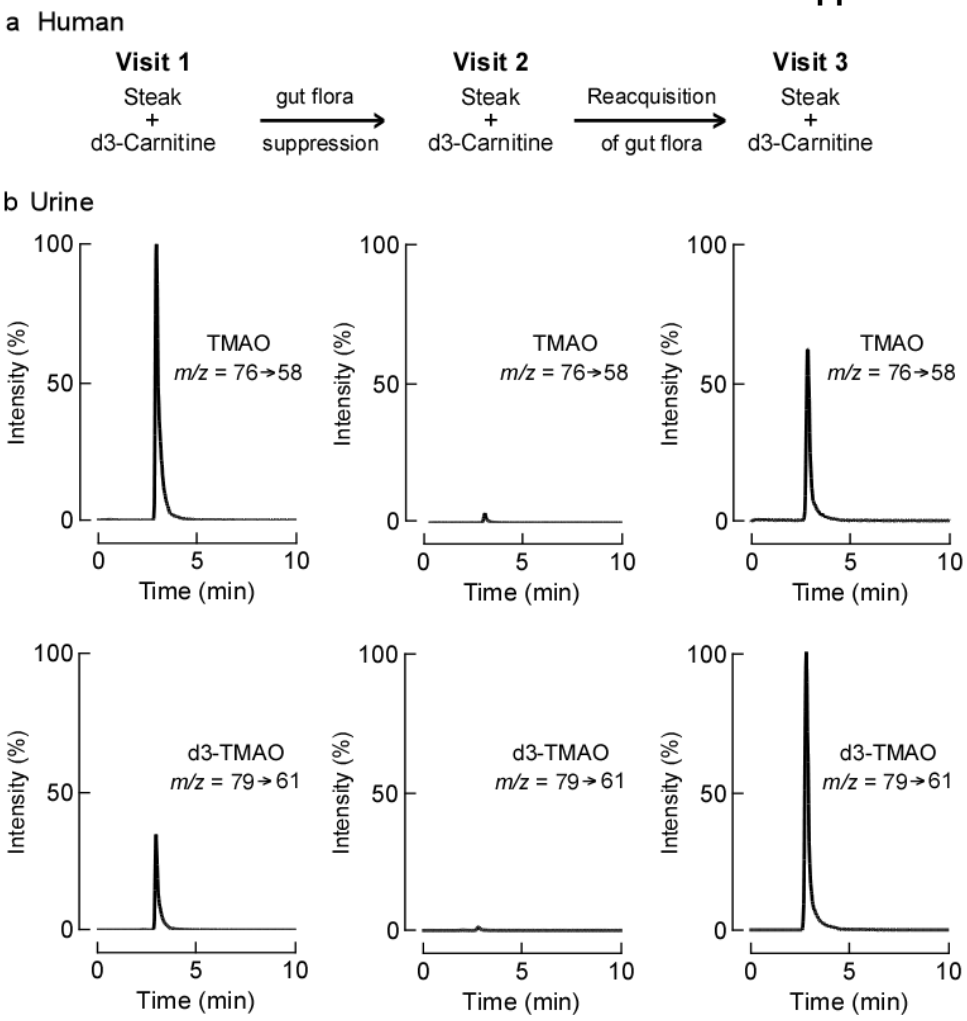


**LC/MS/MS analyses of a subject's 24 hr urine samples demonstrate an obligatory role for gut microbiota in production of TMAO from carnitine.** (**a**) Scheme of overall study. There were 3 visits where carnitine challenge (following overnight fast, ingestion of carnitine in form of 8 oz steak (where indicated) and 250 mg d3-(methyl) carnitine) occurred with serial plasma and 24h urine collection. Visit 1 served as baseline. Subjects then took a cocktail of oral antibiotics for 1 week as described in **Supplementary Methods** to suppress intestinal microbiota, and repeat carnitine challenge was performed at Visit 2. A third and final Visit was performed after at least 1 month of being off of antibiotics. (**b**) Data shown are chromatographic peaks from analysis of urine samples (aliquot of 24 hour collections) from a typical omnivorous subject (from $n > 10$ who underwent carnitine challenge and had complete serial blood draws performed) following carnitine challenge at the indicated visit shown above. The top row of chromatograms is from LC/MS/MS analyses of the indicated precursor $\rightarrow$ product transition specific for TMAO, and the bottom panel represents similar analyses using precursor $\rightarrow$ product transitions specific for d3-TMAO. Note that TMAO and d3-TMAO are readily detected at Visit 1 and 3 after d3-carnitine ingestion, but not Visit 2 where intestinal microbiota is suppressed by oral broad spectrum antibiotics, consistent with a requirement for gut microbiota involvement in both TMA and TMAO formation. Data is organized to vertically correspond with the indicated visit schedule above (Visit 1, 2 or 3).

**Supplementary Figure 5**

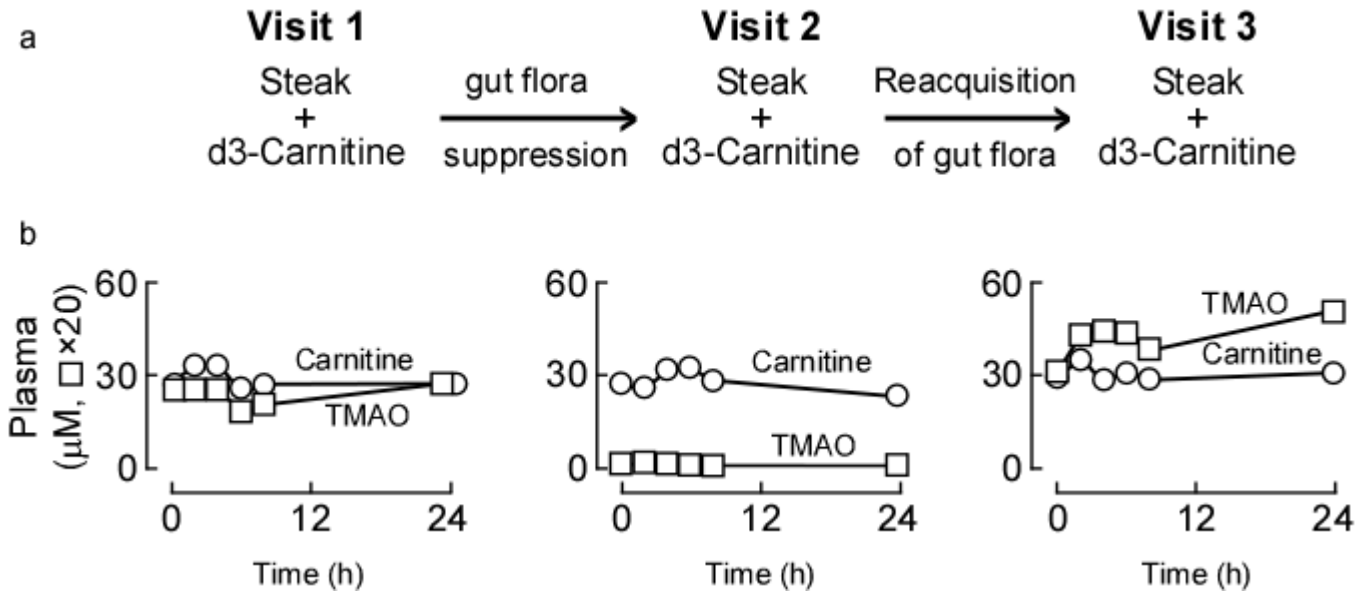


**Plasma levels of carnitine and TMAO following carnitine challenge in a typical omnivorous subject.** (**a**) Scheme of human carnitine challenge test. After an overnight fast, subjects were challenged with a capsule of d3-carnitine (250 mg) alone and with an 8 ounce steak (estimated 180 mg L-carnitine). This was followed with serial plasma and a 24h urine collection for TMAO and carnitine analyses. Visit 2 occurred after a weeklong regimen of oral broad spectrum antibiotics to suppress the intestinal microflora. The challenge was repeated a third time after a ≥ three week period off antibiotics (Visit 3). Data shown (**b**) are from stable isotope dilution LC/MS/MS time course measurements of natural abundance TMAO and carnitine in plasma collected from sequential venous blood draws at noted times from a representative omnivorous subject of n > 10 who underwent carnitine challenge. Data is organized to vertically correspond with the indicated visit schedule above (Visit 1, 2 or 3).

**Supplementary Figure 6**

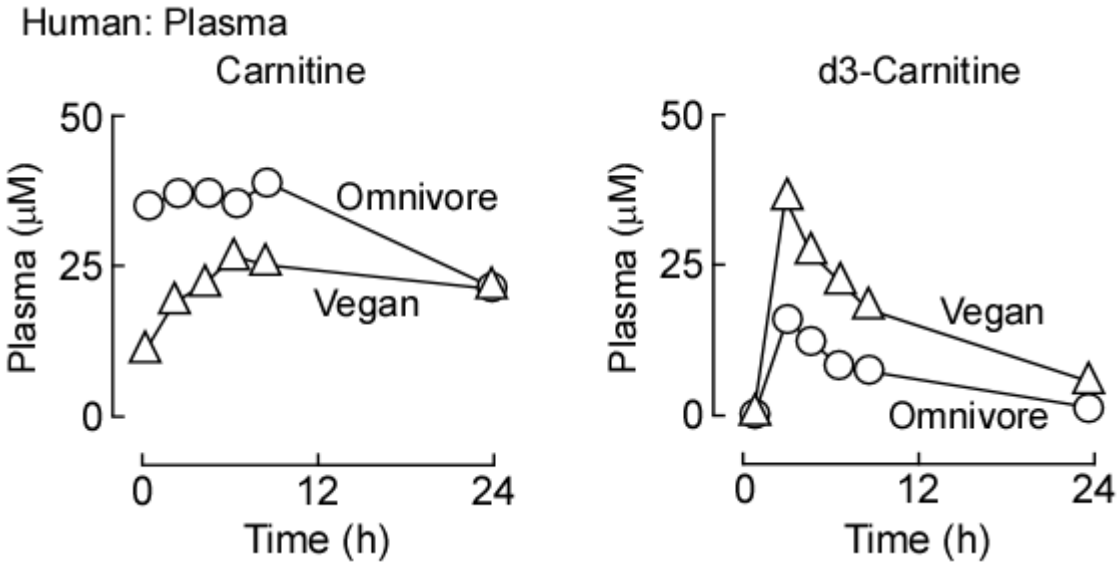


**Plasma levels of carnitine and d3-carnitine following carnitine challenge (steak and d3-carnitine) in typical omnivore with frequent red meat dietary history and a vegan subject.** Plasma was isolated at baseline (T = 0) and the indicated times points following carnitine challenge (8-ounce steak + 250 mg of d3-carnitine) in an omnivore who reported near daily consumption of red meat, and in the one vegan subject who agreed to consume 8 ounces of steak with the d3-carnitine. Plasma levels of endogenous (natural abundance) carnitine (left panel) and the d3-carnitine isotopologue (right panel) were determined by stable isotope dilution LC/MS/MS analysis using synthetic d9-carnitine as internal standard as described in **Supplementary Methods**. The data shown for natural abundance carnitine are typical for the omnivore, where nominal changes in plasma levels are noted following consumption of a steak, but increases from typically relatively lower levels (for vegans/vegetarians) are noted in the vegan subject shown. Substantial increases in the isotope labeled d3-carnitine were found in both vegan and omnivore alike. Also note the greater extent of increase in d3-carntine within the vegan observed compared to the omnivore following ingestion of the d3-carnitine containing capsule, consistent with more intestinal microbiota-mediated catabolism of the d3-carnitine in the omnivore, blunting the amount of carnitine absorbed relative to that observed in the vegan.

**Supplementary Figure 7**

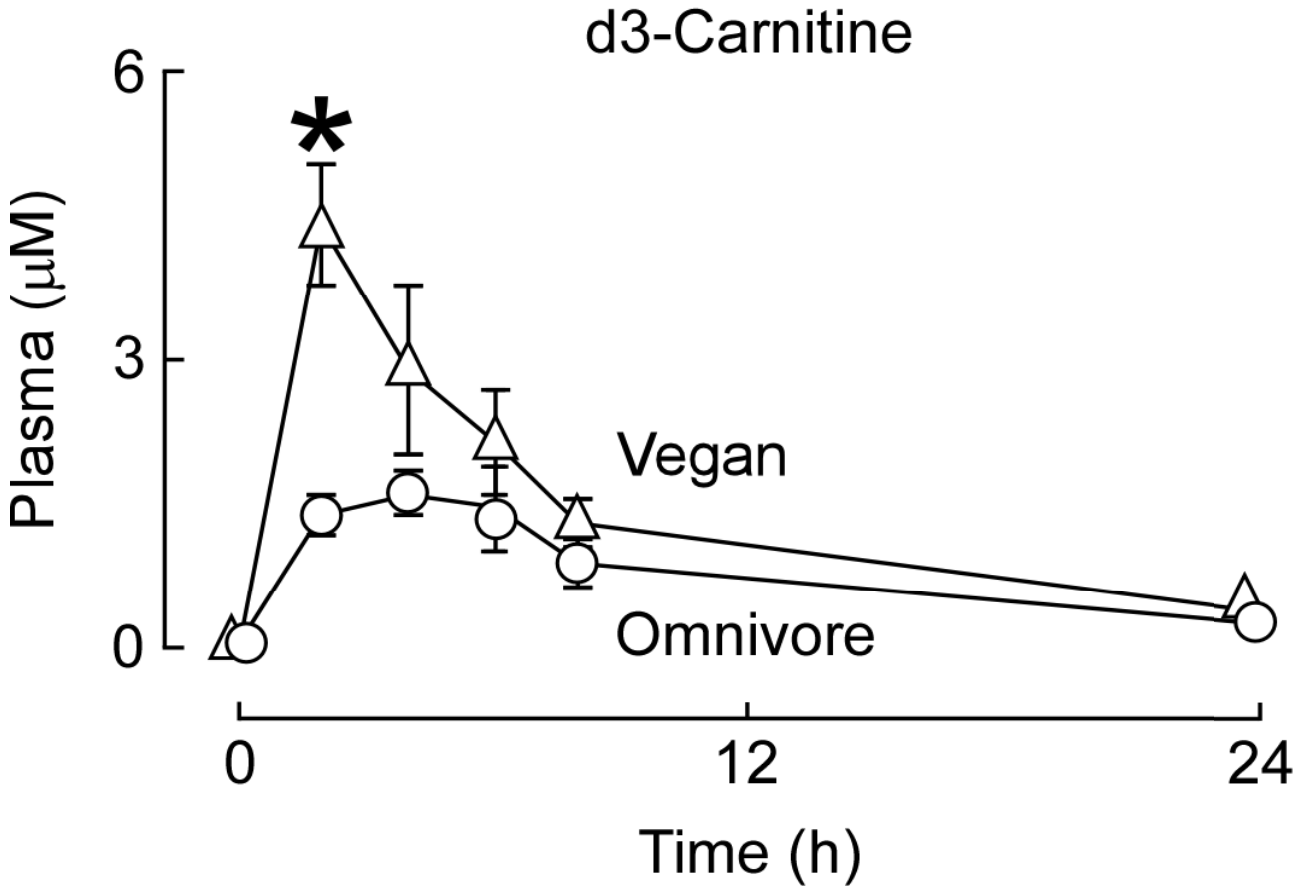


**Plasma levels of d3-carnitine following d3-carnitine challenge (no steak) in omnivorous (*n* = 5) versus vegan subjects (*n* = 5).** Similar studies to that shown in **Supplementary Figure 6** where carnitine challenge did not include ingestion of steak, but only d3-carnitine (250 mg) in a capsule. Plasma was isolated at baseline (T = 0) and the indicated times points following d3-carnitine ingestion in both omnivorous (*n* = 5) and vegan (*n* = 5) subjects. Plasma levels of d3-carnitine were determined by stable isotope dilution LC/MS/MS analysis using synthetic d9-carnitine as internal standard as described in **Supplementary Methods**. Statistical analysis was performed by a Wilcoxon rank-sums test between the mean area under the curve between subjects grouped by omnivorous versus vegan status. A significant increase in plasma d3-carnitine occurs in both vegan and omnivore alike over baseline values, but to a greater extent in vegans, following ingestion of the d3-carnitine containing capsule ($P < 0.05$). This is consistent with more intestinal microbiota-mediated catabolism of the d3-carnitine in the omnivore, blunting the amount absorbed relative to that observed in vegans. * $P < 0.05$ for difference between vegan and omnivore subjects.

**Supplementary Figure 8**

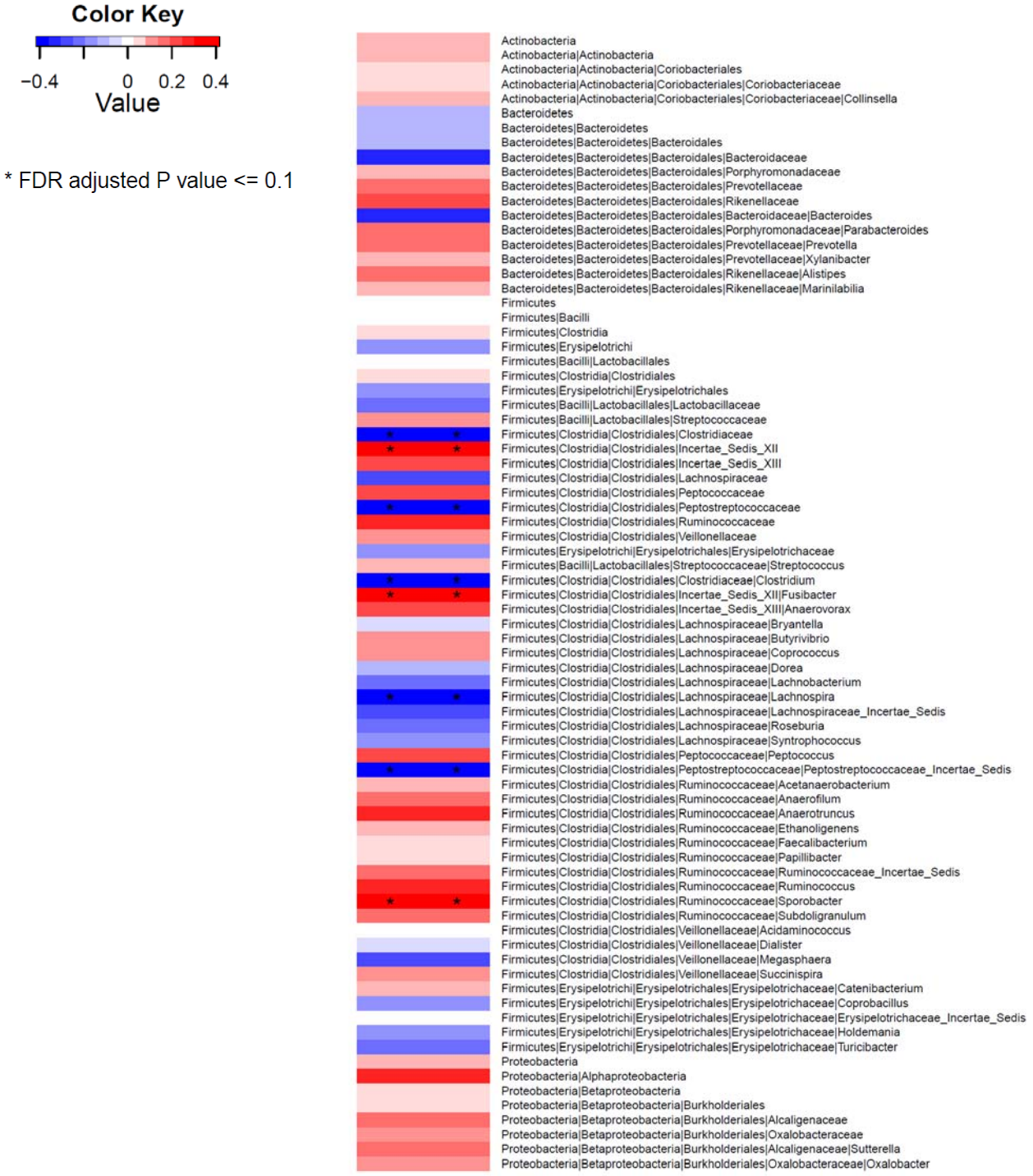


**Human fecal microbiota taxa associate with plasma TMAO.** Human fecal samples were collected from vegan/vegetarians (*n* = 23) and omnivores (*n* = 30) and microbiota gene encoding for 16S rRNA was analyzed as described under **Supplementary Methods**. Associations between plasma TMAO and taxa proportions were assessed as described under **Supplementary Methods**. False discovery rate (FDR) control based on the Benjamini–Hochberg procedure was used to account for multiple comparisons. Asterisked taxa met a FDR adjusted *P* value < 0.1. Further details of the preparation and analysis of human fecal samples can be found in **Supplementary Methods**.

**Supplementary Figure 9**

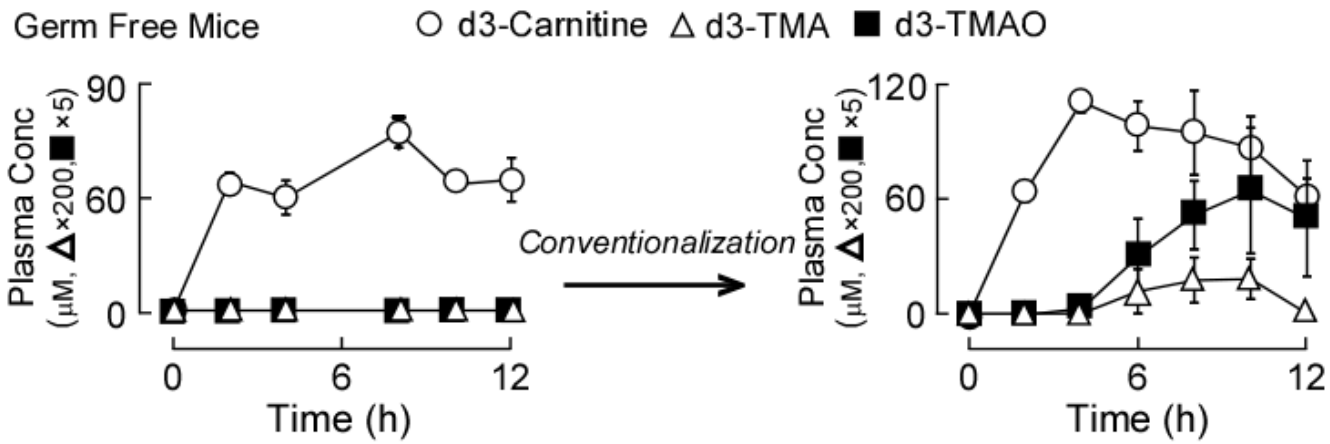


**Demonstration of an obligatory role of the commensal gut microbiota of mice in the production of TMA and TMAO from oral carnitine in germ-free and conventionalized mice**. d3-Carnitine challenge (oral gavage of d3-carnitine) in germ-free female Swiss Webster mice before and after ensuing conventionalization (≥ 3 weeks in conventional cages with conventional mice). Each point represents mean ± SE of 4 independent replicates. Plasma levels of d3-carnitine, d3-TMAO and d3-TMA were determined by stable isotope dilution LC/MS/MS analysis using synthetic d9-(trimethyl)carnitine, d9-(trimethyl)TMA, and d9-(trimethyl)TMAO as internal standards. Note that there is an obligatory role for gut microbiota in generation of TMA and TMAO from orally ingested carnitine, as reflected by the absence of these metabolites in the germ-free mice, but their formation within the conventionalized mice.

**Supplementary Figure 10**

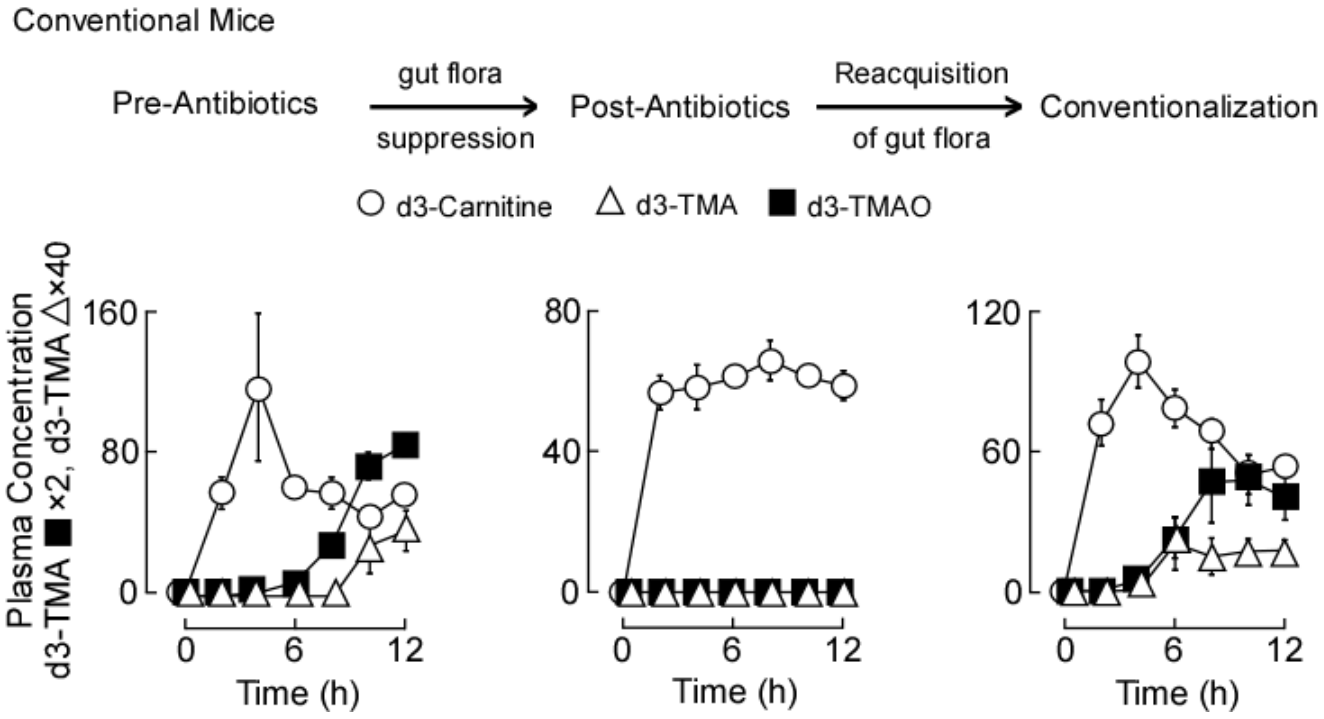


**Demonstration of an obligatory role of commensal gut microbiota of mice in the production of TMA and TMAO from oral carnitine.** Left panel - C57BL/6J, *Apoe*$^{-/-}$ female mice (*n* = 5) in conventional cages were given oral d3-carnitine via gavage at T = 0, and then serial blood draws were obtained at the indicated times. Plasma levels of d3-carnitine, d3-TMAO and d3-TMA were determined by stable isotope dilution LC/MS/MS analysis using synthetic d9-(trimethyl)carnitine, d9-(trimethyl)TMA, and d9-(trimethyl)TMAO as internal standards. Middle panel - Mice were then treated with a cocktail of oral broad spectrum antibiotics to suppress intestinal microbiota as described in **Supplementary Methods**. Repeat gastric gavage with d3-carnitine was performed, and serial testing of plasma for quantification of d3-carnitine, d3-TMA and d3-TMAO levels were determined. Right panel - Antibiotics were stopped and mice allowed to reacquire (≥ 3 weeks) their intestinal microbiota in conventional cages. Repeat gastric gavage with d3-carnitine was performed, and d3-carntine and its metabolites d3-TMA and d3-TMAO were then quantified by LC/MS/MS in serial plasma samples. Results shown are mean ± SE for 5 animals.

**Supplementary Figure 11**

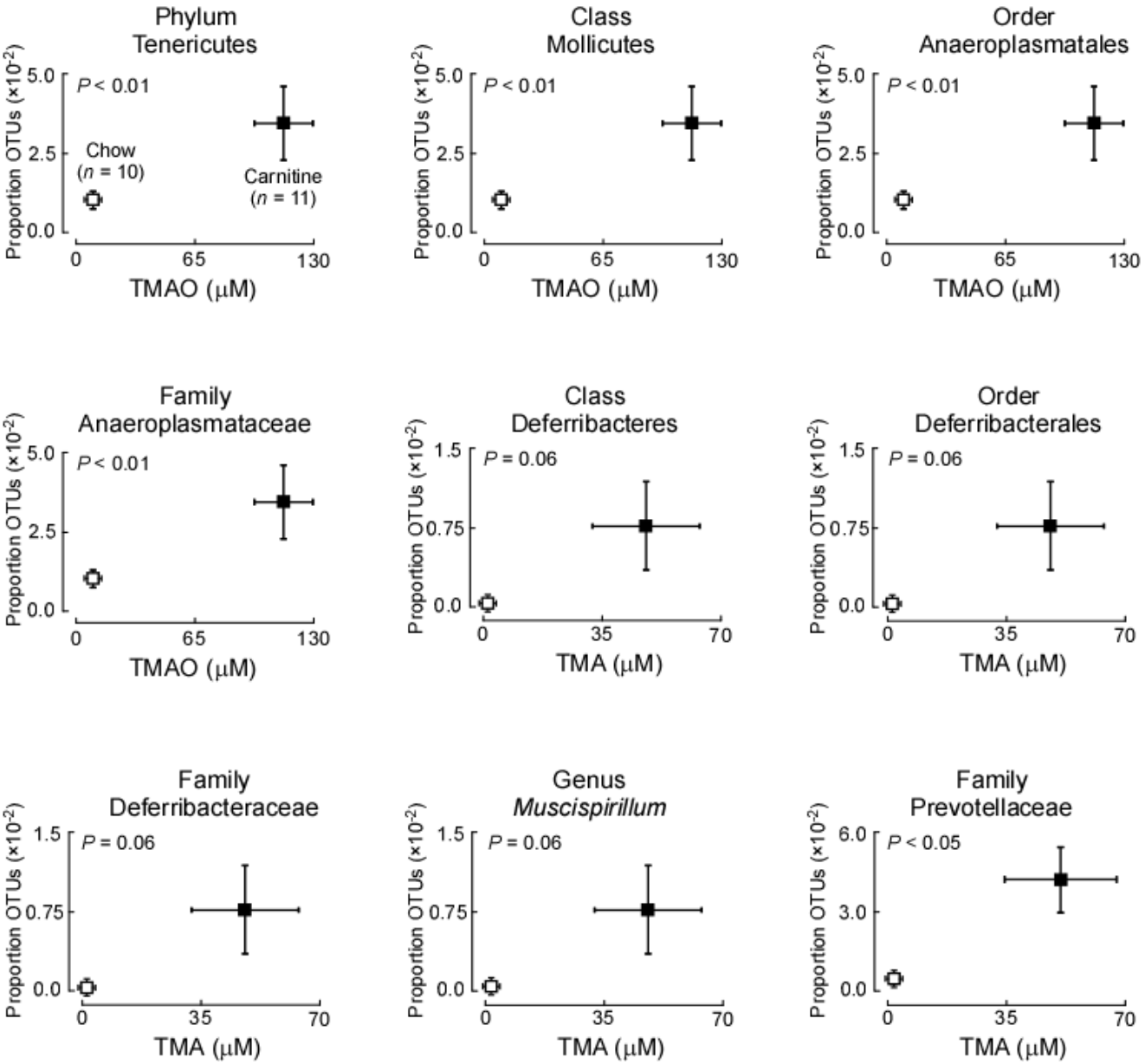


**Analysis of mouse plasma TMA and TMAO concentrations and gut microbiome composition can distinguish dietary status**. C57BL/6J, *Apoe*$^{-/-}$ female mice were maintained either on normal chow ($n$ = 10) or a carnitine supplemented (1.3%) diet ($n$ = 11) as described under **Supplementary Methods**. At sacrifice, blood and intestines were harvested, microbial DNA for the gene encoding 16S-rRNA was isolated from cecal contents, and microbiota composition analyzed as described under **Supplementary Methods**. Plasma TMAO and TMA concentrations were determined by stable isotope dilution LC/MS/MS (plotted on x axes) and the proportion of taxonomic operational units of indicated taxa (OTUs, plotted on Y axes). Analyses and $P$ values shown are for comparisons between dietary groups, and were determined as described in **Supplementary Methods**.

**Supplementary Figure 12**

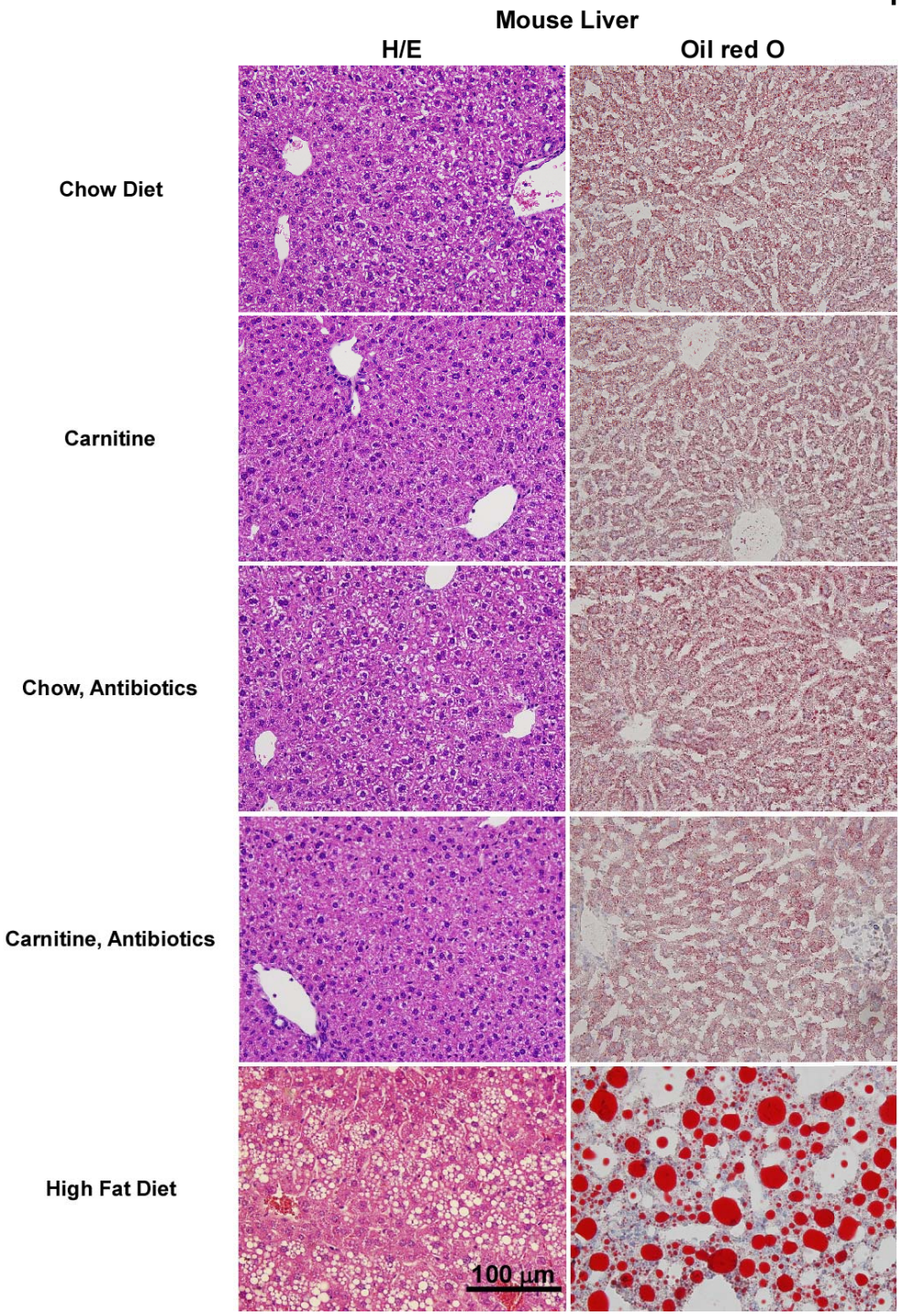


**Haematoxylin/eosin (H/E) and oil-red-O stained liver sections.** Representative liver sections from female C57BL/6J, *Apoe*$^{-/-}$ mice used in atherosclerosis study on the indicated diets collected at time of aorta harvest (19 weeks of age and 15 weeks on diets). Liver was stained by H/E (left column) or oil-red-O and counterstained with Haematoxylin (right column). Mice on these diets exhibit no obvious hepatosteatosis or other pathology. As a positive control for comparison showing fatty liver, C57BL/6J mice fed a high fat diet (16 weeks of age and 6 weeks on the diet) is shown in bottom row.

**Supplementary Figure 13**

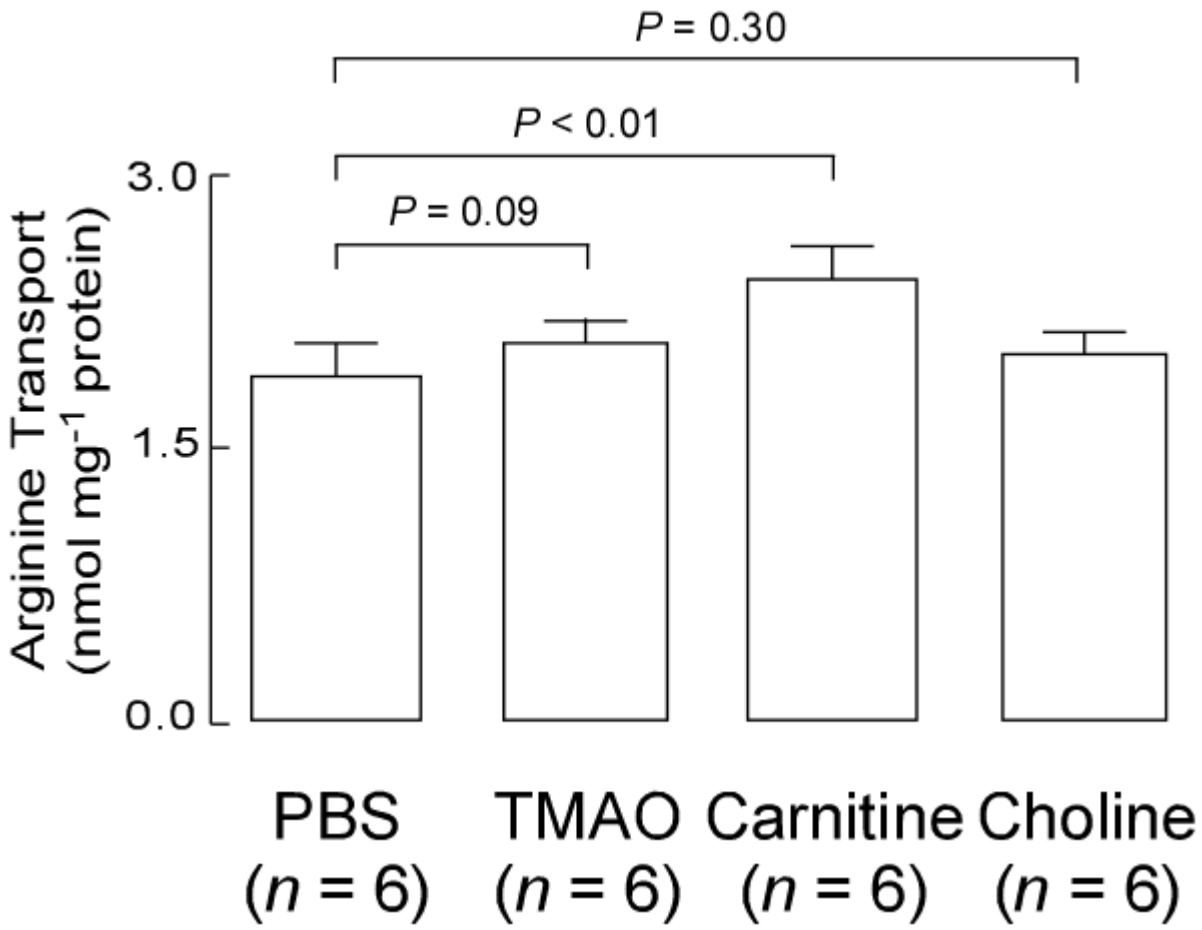


**Arginine transport in the presence of 100 μM trimethylamine-containing compounds.** Bovine aortic endothelial cells (BAEC) were incubated in DMEM medium supplemented with glutamine, 10% FCS and penicillin/streptomycin and with 100 μM of the indicated trimethylamine-containing cationic compounds. BAEC cell arginine uptake studies were performed in Krebs–Henseleit buffer by the addition of 50 μM L-[$^{3}$H] arginine (1 μCi ml$^{-1}$). The samples were incubated for 30 min at 37°C and chased with cold 10 mM L-Arg. After washing with Krebs–Henseleit, the samples were solubilized with 0.1 M NaOH, transferred into plastic liquid scintillation vials and mixed with 4 ml scintillation fluid prior to counting in a Beckman Coulter LS6500 liquid scintillation counter. Data represented mean ± SE from 6 independent replicates. No significant reduction in arginine uptake is noted, suggesting TMAO, carnitine and choline, cationic amino acids, do not compete with arginine for uptake into BAEC.

**Supplementary Figure 14**

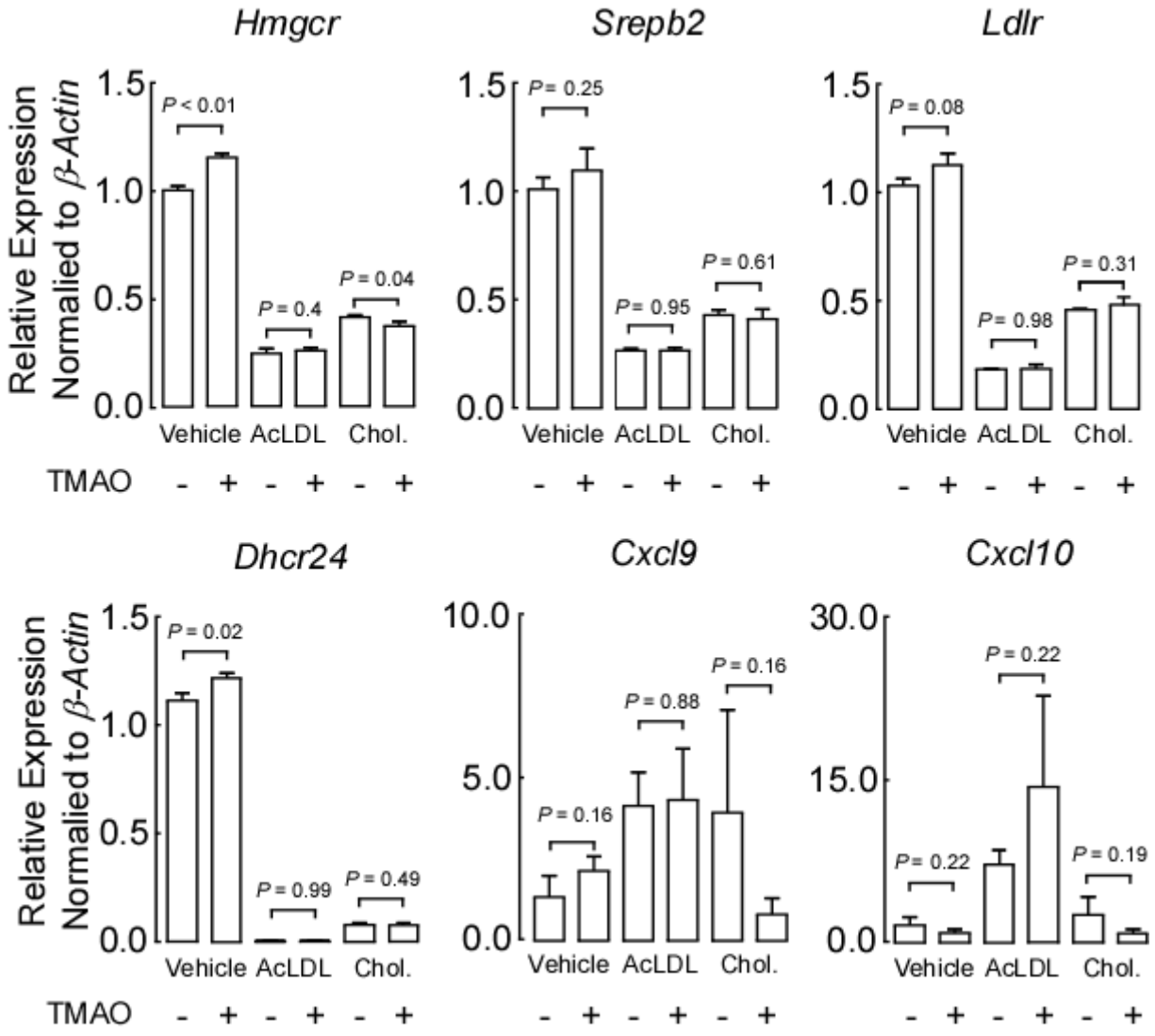


**Expression levels of cholesterol synthesis enzymes, transporters, and inflammatory genes in the presence or absence of TMAO.** Elicited mouse peritoneal macrophages (MPMs) were cultured in RPMI 1640 supplemented with 10% FCS and penicillin/streptomycin overnight. MPMs were then lipoprotein starved in RPMI 1640 supplemented with 10% LPDS and penicillin/streptomycin for 24 hours and then further cultured in the same media for 18 hours in the presence of increasing cholesterol or AcLDL concentrations or vehicle (carrier for AcLDL and cholesterol) with (+) or without (–) 300 μM TMAO (the upper 1% of plasma levels of TMAO noted in the cohort examined in the present study). RNA was then purified, cDNA amplified, and relative (to *β-actin*) expression of the indicated genes quantified by RT-PCR as described in **Supplementary Methods**. Data are expressed as the mean ± SE of $n = 3$ replicates. Differences between conditions + versus – TMAO were evaluated using a student's t-test. Note that no consistent significant effects on candidate gene expression within MPMs in the presence or absence of TMAO are noted. *Hmgcr*, 3-hydroxy-3-methylglutaryl-Coenzyme A reductase; *Srebp2*, sterol regulatory element binding factor 2; Ldlr, low density lipoprotein receptor; *Dhcr24*, 24-dehydrocholesterol reductase; *Cxcl9*, chemokine (C-X-C motif) ligand 9; *Cxcl10*, chemokine (C-X-C motif) ligand 10.

**Supplementary Figure 15**

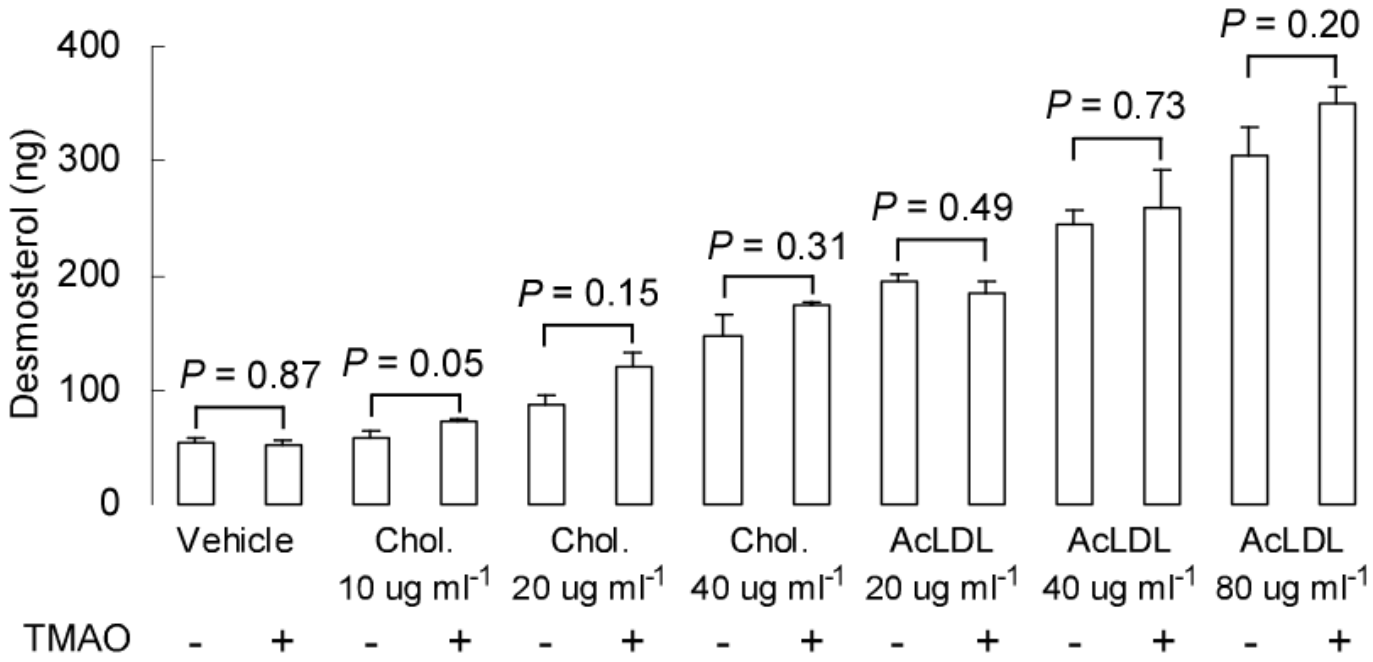


**Effect of TMAO on desmosterol levels in media of cultured mouse peritoneal macrophages in the presence of increasing cholesterol and acetylated LDL (AcLDL) concentrations.** Elicited mouse peritoneal macrophages (MPMs) were cultured in RPMI 1640 supplemented with 10% FCS and penicillin/streptomycin overnight. MPMs were then lipoprotein starved in RPMI 1640 supplemented with 10% LPDS and penicillin/streptomycin for 24 hours and then further cultured in the same media for 18 hours in the presence of increasing cholesterol and AcLDL concentrations or vehicle (carrier for AcLDL and cholesterol) with (+) or without (–) 300 μM TMAO. Media was harvested and the content of desmosterol was determined as described under **Supplementary Methods**. Data represented mean ± SE from 3 independent replicates.

**Supplementary Figure 16**

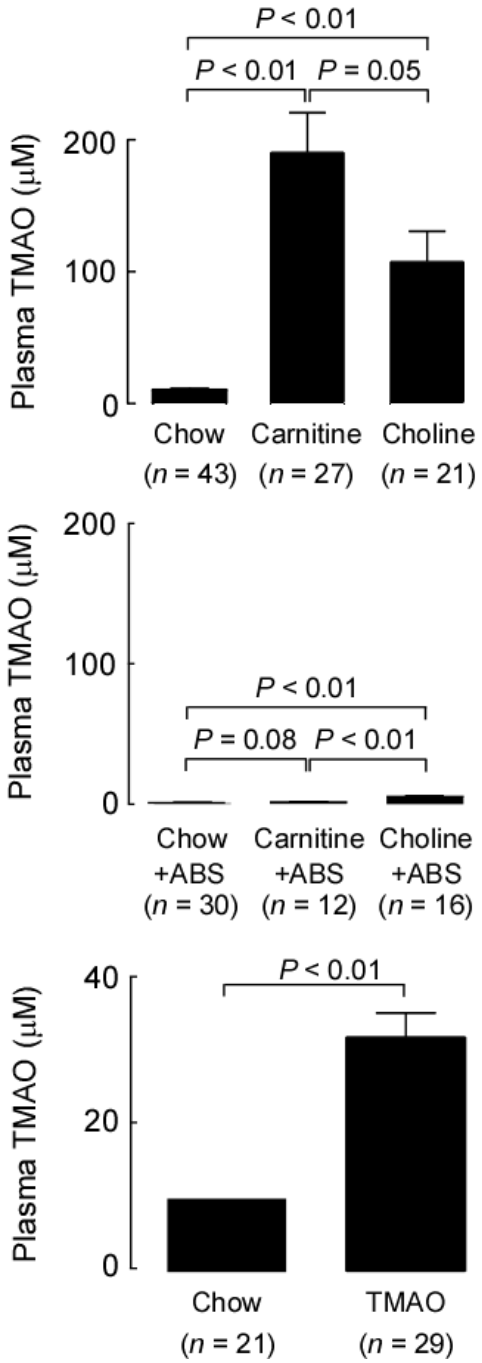


**Plasma concentrations of TMAO in mice undergoing *in vivo* reverse cholesterol transport studies.** Adult (> 8 weeks of age) C57BL/6J, *Apoe*$^{-/-}$ female mice were placed on normal chow or either carnitine (1.3%) or choline (1.3%) supplemented diets. Where indicated, some groups of mice also had addition of a cocktail of antibiotics to their drinking water as described under **Supplementary Methods** throughout the duration of the dietary feeding period and RCT study. TMAO concentration was determined by stable isotope dilution LC/MS/MS analysis of plasma recovered from mice at time of sacrifice in the reverse cholesterol transport studies. A Wilcoxon non-parametric test was used to assess the difference in plasma TMAO between animal diets. Data shown are mean ± SE.

**Supplementary Figure 17**

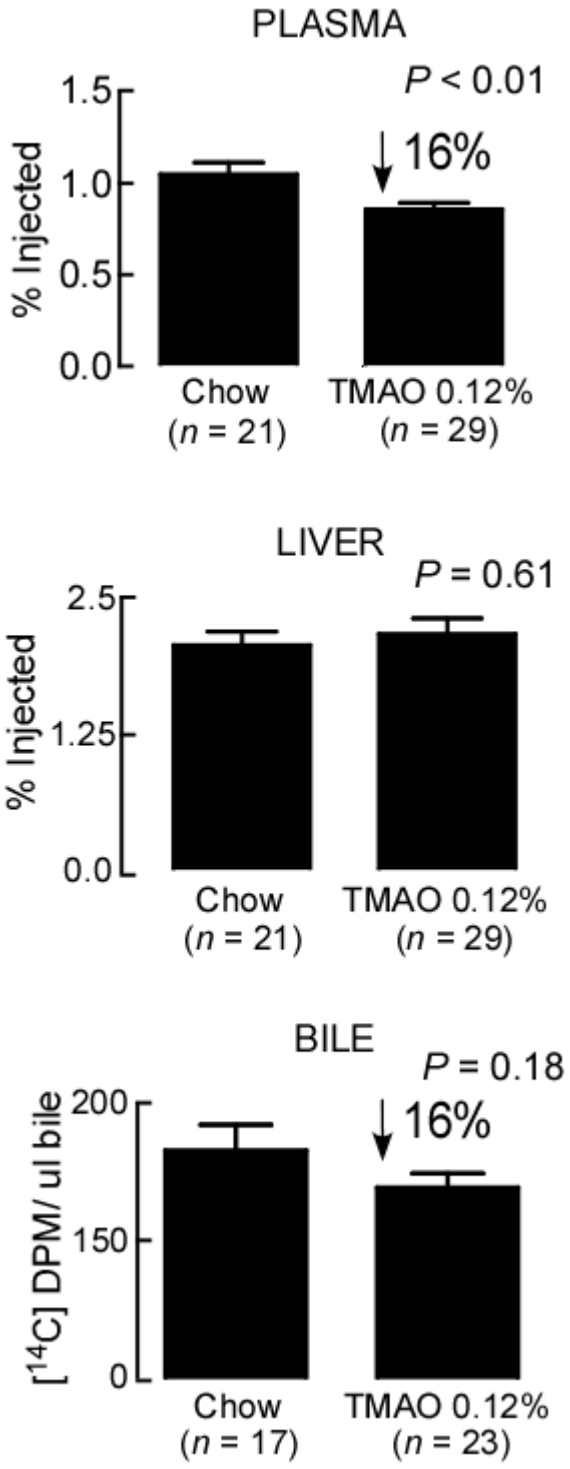


**[$^{14}$C] Cholesterol recovered from mice on normal chow vs. TMAO diet enrolled in *in vivo* reverse cholesterol transport studies.** Adult (> 8 weeks of age) C57BL/6J, *Apoe*$^{-/-}$ female mice were placed on either normal chow or a TMAO (0.12%) supplemented diet for 4 weeks before performing *in vivo* reverse cholesterol transport studies as described under **Supplementary Methods**. Mice were sacrificed 72 hours post injection with [$^{14}$C]cholesterol-loaded bone marrow-derived macrophages and counts within plasma, liver, and bile were determined as described in **Supplementary Methods.** Results shown are mean ± SE.

**Supplementary Figure 18**

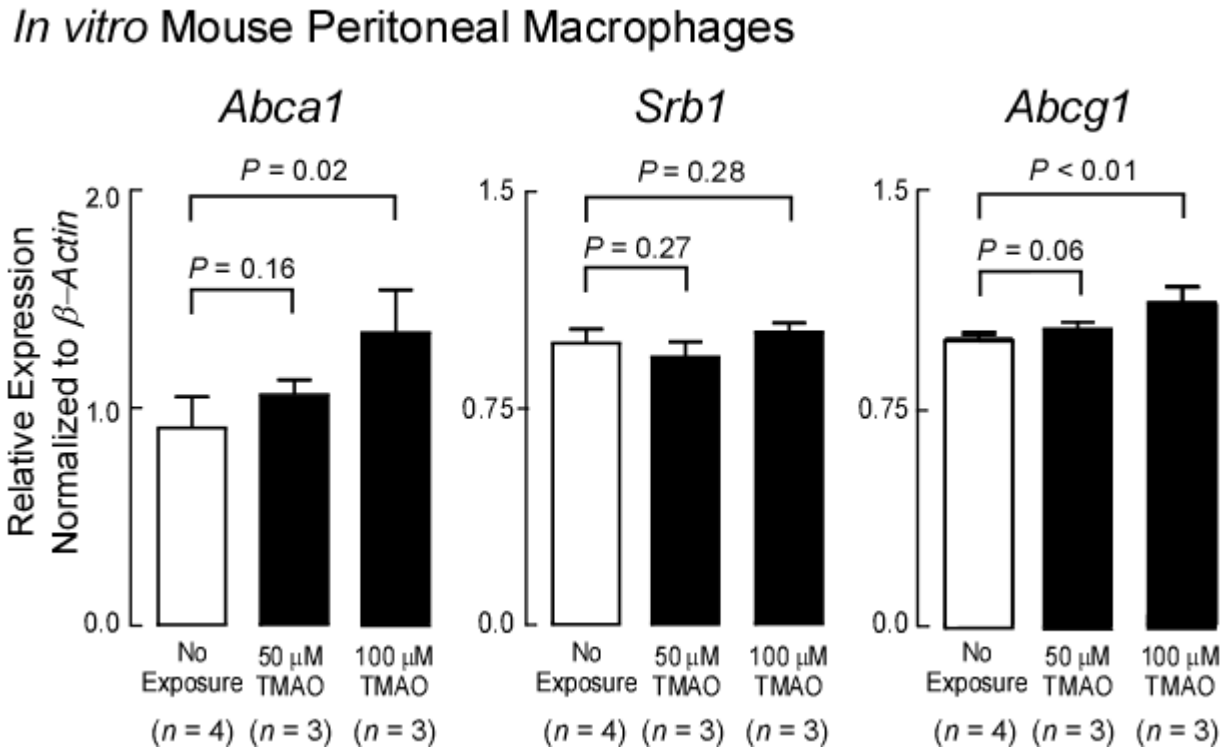


**Effect of TMAO on mouse peritoneal macrophages.** Thioglycollate elicited mouse peritoneal macrophages (MPMs) from C56Bl/6J mice were cultured in RPMI media supplemented with 5% lipoprotein deficient serum, glutamine, and penicillin and streptomycin. MPMs were then further incubated in the same media for an additional 20 hours with the indicated levels of TMAO. RNA was then purified, cDNA amplified, and relative (to *β-actin*) expression of the indicated genes quantified by RT-PCR as described in **Supplementary Methods**. Data are expressed as the mean ± SE.

**Supplementary Figure 19**

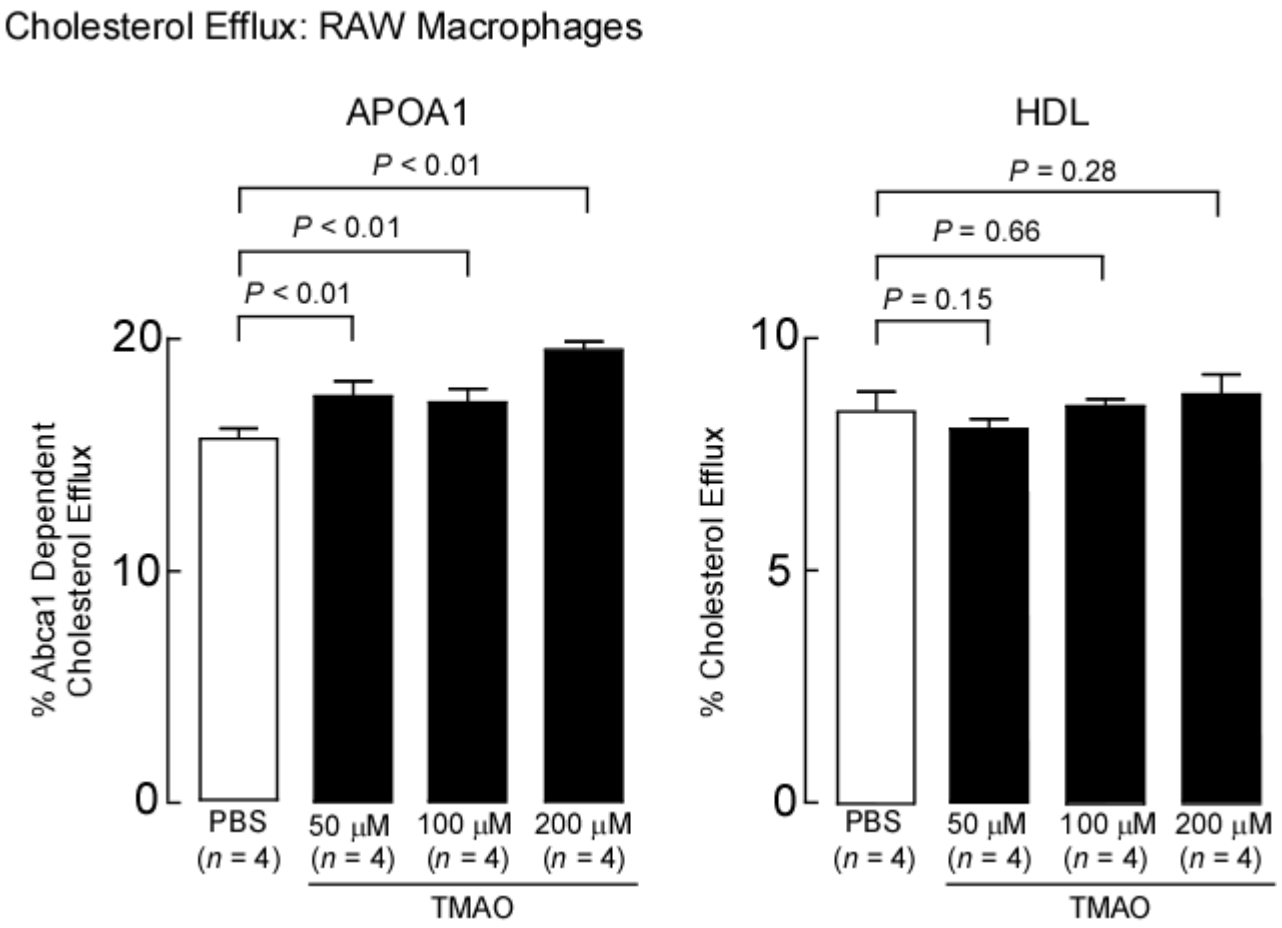


**Effect of TMAO on cultured macrophage cholesterol efflux.** RAW264.7 macrophages were cultured in DMEM media supplemented with 10% FBS and penicillin/streptomycin until 75% confluence. Cells were then further incubated in DMEM media supplemented with 12.5 g $l^{-1}$glucose, 200 mM glutamine, 1.25 g $l^{-1}$ BSA, and penicillin/streptomycin + or – cyclic AMP (for *Abca1* expression induction) for an additional 16 hours with the indicated levels of TMAO. Abca1-dependent and total cholesterol efflux were then determined using lipid free isolated human apolipoprotein A1 (APOA1), or isolated human HDL, as cholesterol acceptor, as described in **Supplementary Methods.** Data are expressed as the mean and ± SD of replicates (*n* = 4). A student's t-test was used to assess the relative increase in cholesterol efflux relative to a PBS (no exposure) control. While a statistically significant increase in Abca1-dependent cholesterol efflux in macrophages exposed to TMAO is noted ($P < 0.01$), the biological significance is unclear given the modest level of the effect, even at the highest levels of TMAO used.

**Supplementary Figure 20**

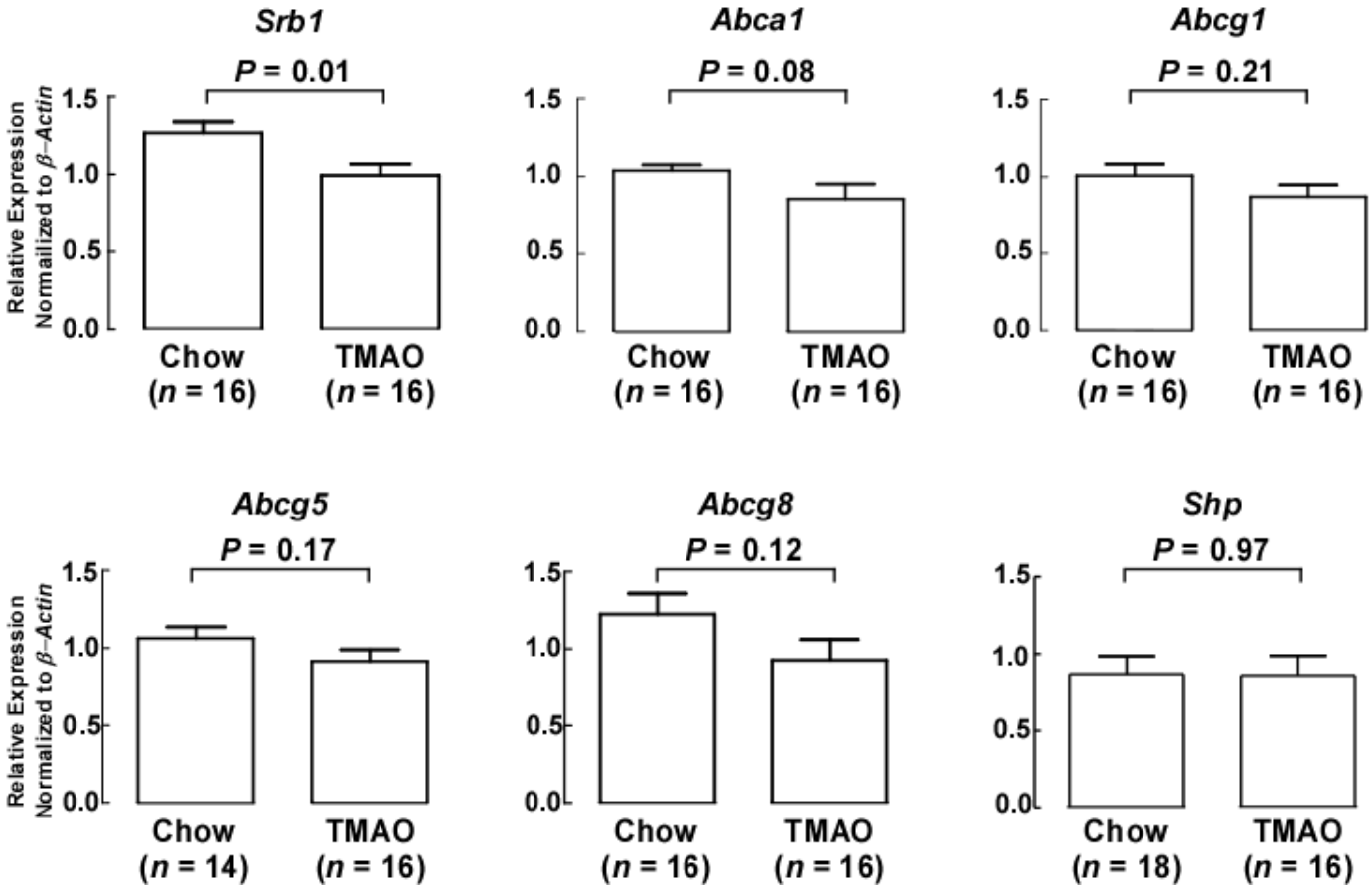


**Liver expression of cholesterol transporters in mice examined during reverse cholesterol transport studies.** Livers from C57BL/6J, *Apoe*$^{-/-}$ female mice on the indicated diets in the reverse cholesterol transport experiments were collected at time of sacrifice. The relative expression levels of the indicated genes were determined by RT-PCR as described in **Supplementary Methods.** Data are presented as mean ± SE.

**Supplementary Figure 21**

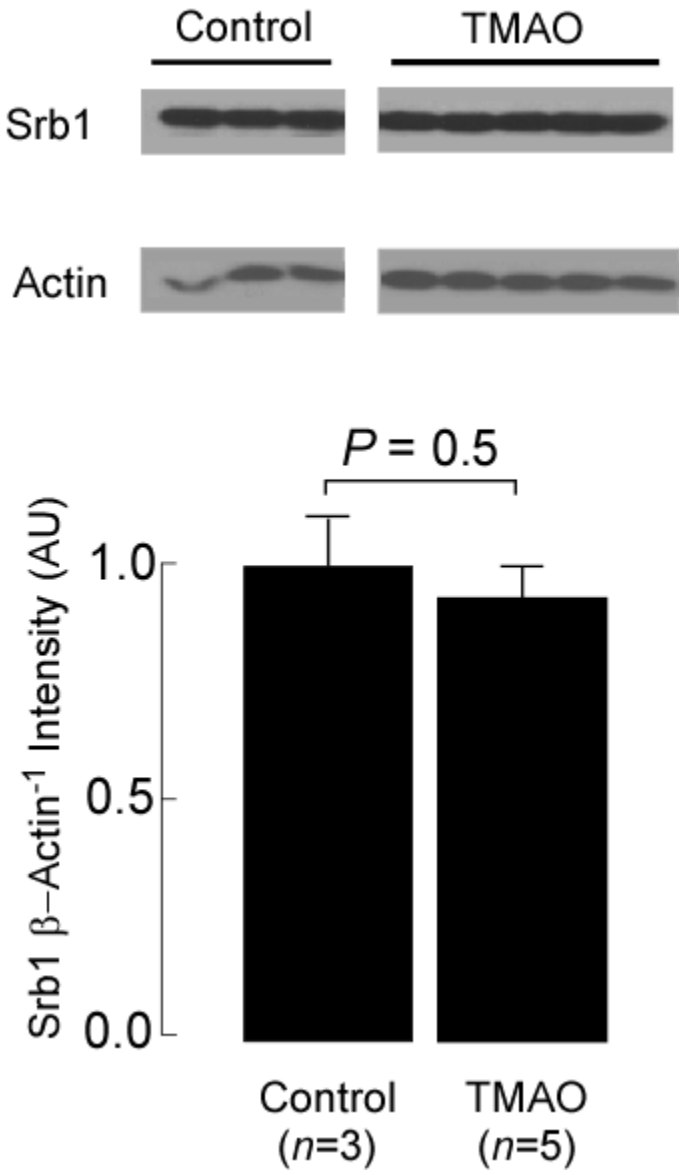


**Western blot analysis of liver scavenger receptor B1 (Srb1) expression.** Female C57BL/6J*, Apoe*$^{-/-}$ mice were placed on either normal chow or diet supplemented with TMAO (0.12%) at time of weaning, and then lever harvested at time of sacrifice (20 weeks of age). Mouse liver lysate (30 µg protein) was run on SDS PAGE and then transferred to PVDF membrane. The membranes were probed with antibodies against Srb1 (Novus, Littleton, CO) and β-actin (Sigma, St. Louise, MO), and intensity of bands quantified by densitometry using ImagePro Plus software. Data are expressed as means ± SE.

**Supplementary Figure 22**

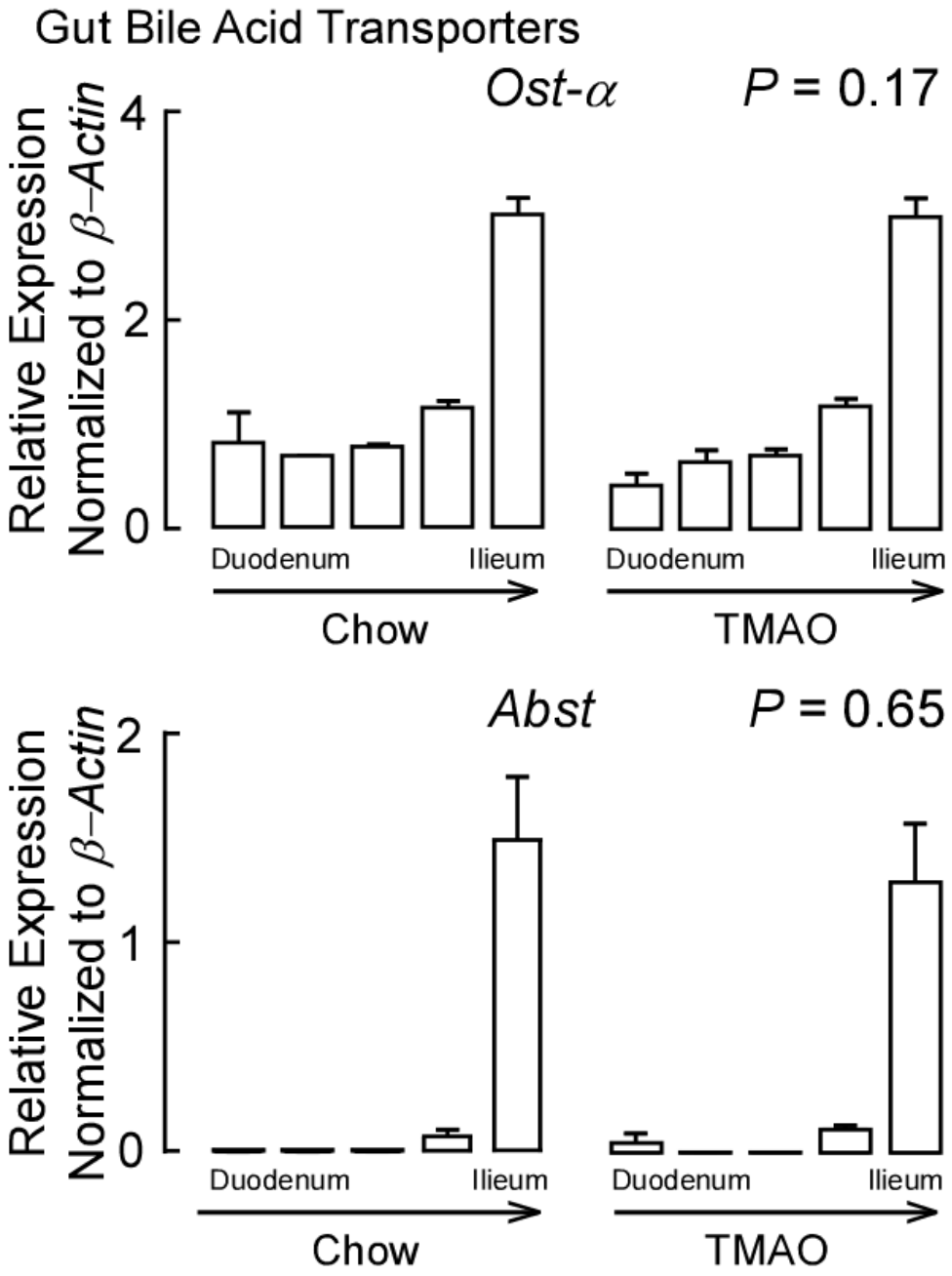


**Small intestines expression profile of bile acid transporters in mice.** Intestines from C57BL/6J*, Apoe*$^{-/-}$ female mice on the indicated diets enrolled in the *in vivo* reverse cholesterol transport experiments were harvest at completion of the study en-block. The small intestines were resected, extended lengthwise, and divided into 5ths. Tissue RNA was isolated from each segment and relative expression (to *β-actin*) of the indicated genes determined by RT-PCR as described in **Supplementary Methods.** Data are expressed as mean ± SE. Note that there is no statistically significant differences noted in the expression pattern of the monitored genes along the length of the small intestines when comparing the pattern in chow vs. TMAO dietary groups of animals, as assessed by ANOVA. *Ost-α*; solute carrier family 51, alpha subunit; *Asbt*, solute carrier family 10, member 2.

**Supplementary Figure 23**

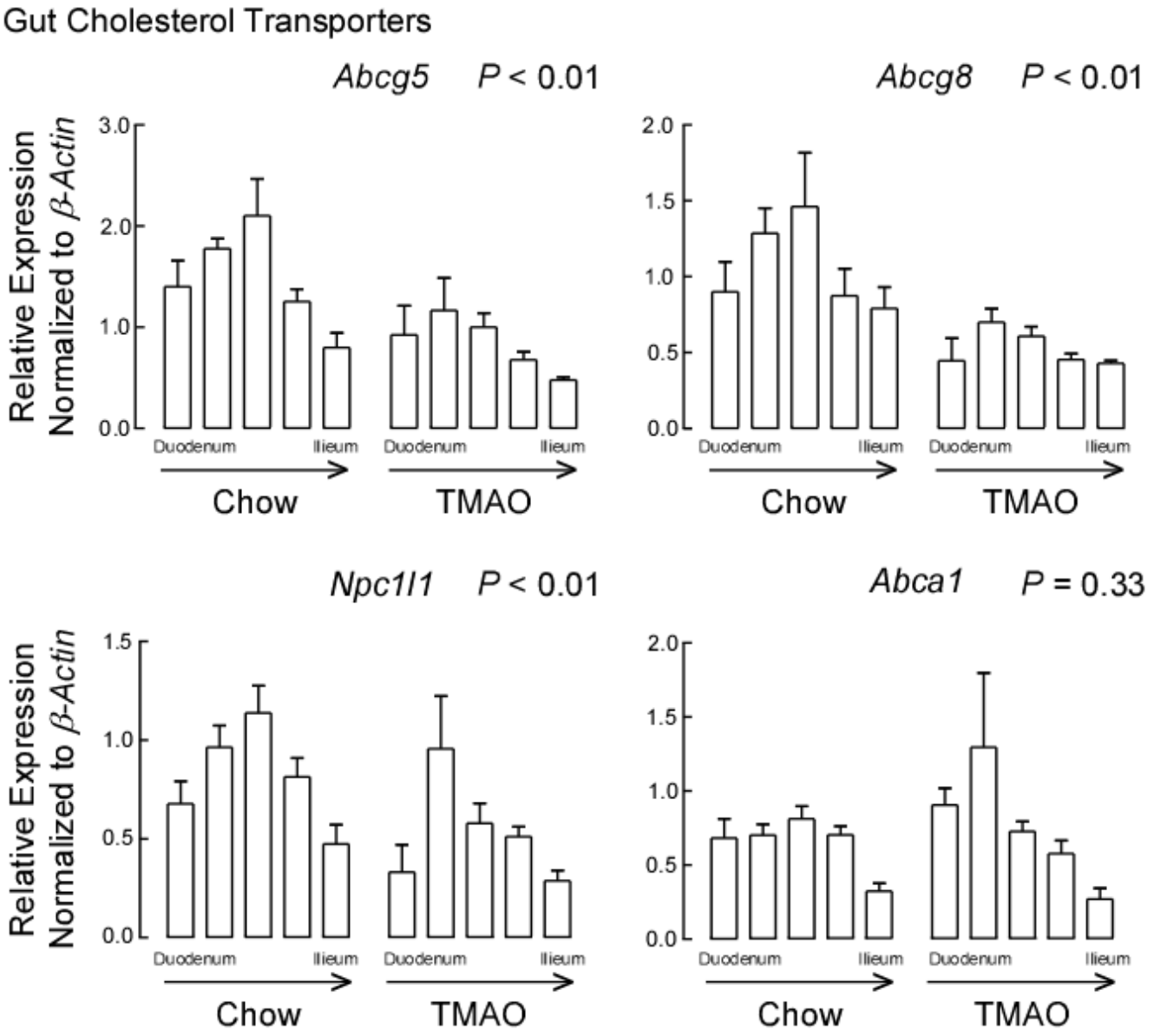


**Small intestines expression profile of cholesterol transporters in mice.** Intestines from C57BL/6J*, Apoe*$^{-/-}$ female mice on the indicated diets enrolled in the *in vivo* reverse cholesterol transport experiments were harvest at completion of the study en-block. The small intestines were resected, extended lengthwise, and divided into 5ths. Tissue RNA was isolated from each segment and relative expression (to β actin) of the indicated genes determined by RT-PCR as described in **Supplementary Methods.** Data are expressed as mean ± SE. P values for differences in the distribution of expression patterns of the monitored genes along the length of the small intestines when comparing the chow vs. TMAO dietary groups of animals were assessed by ANOVA.

## Supplementary Methods

### Materials and general procedures

Mouse HDL cholesterol was determined enzymatically (Stanbio Laboratory, Boerne, TX) from mouse plasma HDL isolated using density ultracentrifugation. Mouse plasma insulin measurements were performed using the Mercodia Mouse Insulin Elisa Kit (Uppsala, Sweden). Liver triglyceride content was quantified by GPO reagent (Pointe Scientific, Canton, MI) and normalized to liver weight in grams as described[2]. Liver cholesterol was quantified in liver homogenates in which coprostanol (Steraloids, Inc, Newport, RI) was added as an internal standard, lipids extracted by the Folch method (chloroform:methanol (2:1, v/v)), and then cholesterol quantified as its trimethylsilane (TMS) derivative (Sylon HTP, Sigma-Aldrich, Sigma St. Louis, MO) by GC/MS (Agilent 5973N model, Santa Clara CA) on a DB-1 column (12m x 0.2 mm diameter x 0.250um film thickness)[3,4].

### Cardiovascular research subjects

Studies assessing the relationship between plasma carnitine levels and both prevalent and incident cardiovascular risks were performed using archival specimens from the study GeneBank, a research repository (*n* = 2,595) comprised of sequential consenting stable subjects undergoing elective cardiac evaluation and who were subsequently followed longitudinally for incident cardiovascular disease (CVD) outcomes[1,5]. Patients with a recent (< 4 weeks) clinical history of myocardial infarction or elevated troponin I (> 0.03 md $dl^{-1}$) at enrollment were excluded from the study. CVD was clinically defined as having a previous history of coronary artery disease (CAD), peripheral artery disease (PAD), and/or cerebral vascular disease (history of a transient ischemic attack or cerebrovascular accident), history of revascularization (coronary artery bypass graft, angioplasty, or stent) or significant angiographic evidence of CAD (≥50% stenosis) in at least one major coronary vessel. Subjects with CAD included patients with adjudicated diagnoses of stable or unstable angina, myocardial infarction, history of coronary revascularization, or angiographic evidence of ≥50% stenosis of one or more major coronary arteries. PAD was defined as subjects having clinical evidence of extra-coronary atherosclerosis. Medications were documented by patient interview and chart review.

### Metabolomics study

In a previous study we reported results from a metabolomics study in which small molecule analytes were sought that associated with cardiovascular risks[1]. Analytes were only known for their mass-to-charge ratio (*m/z*) and retention time, with identities unknown. Analytes considered of interest in the metabolomics studies were selected based on the following criteria: (i) the unknown analyte had a significant difference ($P < 0.05$) between cases and controls in the Learning and Validation Cohorts after a two sided Bonferroni adjusted t-test; (ii) the unknown analyte had a significant ($P < 0.05$) dose-response relationship between analyte peak area and major adverse cardiovascular event risk using an unadjusted log-rank test of trend; and (iii) to facilitate future quantification and structural identification efforts, analytes had to have a signal-to-noise ratio of 5:1 in at least 75% of subjects within cases and controls of both the Learning and Validation Cohorts as previously described[1].

While an ion with *m/z* and retention time identical to carnitine was not amongst the top analytes identified in the above metabolomics studies, we attempted for the present studies to examine the original data, this time using less stringent criteria, with the hypothesis-generated focus of examining just the single ion that had chromatographic and mass spectral characteristics observed identical with standard L-carnitine: namely, *m/z* = 162 and appropriate retention time. Examination of **Supplementary Table 1** shows that an analyte with appropriate *m/z* and retention time in the Learning and Validation Cohorts was observed that failed to meet significance using the originally used stringent criteria (the more strict Bonferroni adjusted *p* value). However, reexamination of the combined Learning and Validation cohorts ($n = 75$ cases, $n = 75$ controls) without adjustment for multiple testing (since only one analyte here was being screened for) showed the unknown analyte with *m/z* = 162 and retention time identical to carnitine was associated with atherosclerotic disease outcomes.

**Identification of L-carnitine and d9-carnitine preparation**

Matching CID spectra of the unknown metabolite of interest with a precursor ion at *m/z* = 162 and authentic L-carntine standard were examined using a Cohesive Technologies Aria HPLC interfaced to a AB Sciex API 5000 triple quadrupole mass spectrometer (Applied Biosystems) in positive ion mode by a method described previously[1]. Mouse and human samples were also spiked with synthetic d9(trimethyl)-carnitine as internal standard. Samples were analyzed using a similar system as above

except a Shimadzu (Columbia, MD) dual gradient HPLC system was interfaced to the AB Sciex API 5000 tandem mass spectrometer. Multiple distinct parent → product ion transitions specific for the natural abundance and d9-isotopologue of carnitine were monitored simultaneously in the spiked sample, to determine if multiple characteristic MRM channels for each isotopologue of carnitine were present and co-chromatographed.

Synthesis of the d9-carnitine standard for the above experiment, and for use as internal standard in stable isotope dilution LC/MS/MS analyses of carnitine and synthetic d3-carnitine following a carnitine challenge, were prepared and characterized as follows: First, 3-hydroxy-4-aminobutyric acid (Chem-Impex Intl.) was dissolved in methanol and reacted with d3-methyl iodide (Cambridge Isotope Labs, Boston, MA) in the presence of potassium hydrogen carbonate to give d9-carnitine, as per Chen and Benoiton[6]. The d9-L-carnitine was isolated by passing the reaction mixture directly over a silica gel column rinsing with additional methanol, and then eluting the heavy isotope labeled L-carnitine with 30% v/v water in methanol. The product was dried via azeotropic distillation of absolute ethanol and subsequently recrystallized from ethanol and acetone. The white to off-white crystalline product was dried over $P_2O_5$ *in vacuo* and stored refrigerated. TLC on silica gel eluted with methanol plus 0.2%v/v formic acid visualized by iodine staining showed one spot with the same Rf as L-carnitine. The mass spectrum of the compound dissolved in 50% v/v methanol / water (5 mM formic acid) to a concentration of 50 μg $ml^{-1}$ exhibited a base peak at *m/z* = 171 in the positive ion mode corresponding to [M]+. CID fragments peaks were observed at *m/z* = 111,103, 85, 69, 57, and 43. Mass spectral fragmentation patterns and *m/z* ratios are consistent with the L-carnitine except for those fragment ions that contain the trimethylammonium group; these ions exhibit fragments 9 atomic mass units (amu) higher than the corresponding signals from L-carnitine due to the incorporation of 9 deuterium atoms on the methyl groups attached to the nitrogen.

**Quantification of TMAO, TMA, and L-carnitine**

Stable isotope dilution LC/MS/MS was used to quantify TMAO, TMA and L-carnitine from acidified plasma samples in positive MRM mode. Precursor → product ion transitions at *m/z* 76 to 58, *m/z* 162 to 60 and *m/z* 60 to 44 were used for TMAO, L-carnitine, and TMA respectively. As internal standards, d9(trimethyl)TMAO (d9-TMAO), d9(trimethyl)carnitine (d9-carnitine), and d9(trimethyl)TMA (d9-TMA)

were added to mouse and human plasma samples for their respective native compounds. Increasing concentrations of L-carnitine, TMA and TMAO standards with a fixed amount of internal standard were added to human control plasma to generate calibration curves for determining plasma concentrations of each analyte, using methods similar in approach to that previously described[1], with samples run on an AB Sciex API 5000 triple quadrupole mass spectrometer.

**Mouse microbiota analysis**

Barcoded primers were achieved following the protocol described by Hamady et al[7]. Sample preparation was performed similarly to that described by Costello et al.[8]. Each sample was amplified in triplicate, combined in equal amounts and cleaned using the PCR clean-up kit (Mo Bio, Carlsbad, CA). Cleaned amplicons were quantified using Picogreen dsDNA reagent (Invitrogen, Grand Island, NY) before sequencing using 454 GS FLX titanium chemistry at the EnGenCore Facility at the University of South Carolina. The raw data from the 454 pyrosequencing machine were first processed through a quality filter that removed sequence reads that did not meet the quality criteria. Sequences were removed if they were shorter than 200 nucleotides, longer than 1,000 nucleotides, contained primer mismatches, ambiguous bases, uncorrectable barcodes, or homopolymer runs in excess of six bases. The remaining sequences were analyzed using the open source software package Quantitative Insights Into Microbial Ecology (QIIME[9,10]). A total of 11519 quality filtered reads were obtained from 23 samples (1 sample was removed due to low number of sequences). Individual reads that passed filtering were distributed to each sample based on bar-code sequences. De-multiplexed sequences were assigned to operational taxonomic units (OTUs) using UCLUST with a threshold of 97% pair-wise identity. Representative sequences were selected and BLASTed against a reference Greengenes reference database. For each resulting OTU, a representative sequences were selected by choosing the most abundant sequence from the original post-quality filtered sequence collection. The taxonomic composition was assigned to the representative sequence of each OTU using Ribosomal Database Project (RDP) Classifier 2.0.1[11] The relative abundances of bacteria at each taxonomic level (e.g., phylum, class, order, family and genus) were computed for each mouse. For tree-based analyses, a single representative sequence for each OTU was aligned using PyNAST[12], then a phylogenetic tree was built using FastTree. The phylogenetic tree was used to

measure the β-diversity (using unweighted UniFrac) of samples[13]. Two-way ANOVAs were conducted to evaluate the effects of diet with *P* values corrected for multiple comparisons. Spearman correlations between relative abundance of gut microbiota and TMA and TMAO levels and association testing were performed in R. False discovery rates (FDR) of the multiple comparisons were estimated for each taxon based on the *P*-values resulted from correlation estimates.

**d3-L-Carnitine preparation**

Synthesis of d3-L-carnitine for carnitine challenge tests was prepared and characterized as follows: L-Norcarnitine (3-hydroxy-4-dimethylaminobutyric acid) was prepared from L-carnitine (Chem Impex International, Woodale, IL) with thiophenol (Sigma Aldrich Milwaukee, WI) in N,N-dimethylaminoethanol (Sigma Aldrich Milwaukee, WI) and subsequently converted to its sodium salt with sodium hydroxide by the method of Colucci, et. al.[14]. Sodium L-norcarnitine was recrystallized three times from ethanol and 3 volumes of ethyl acetate prior to the subsequent conversion to d3-L-carnitne. TLC on silica gel eluted with methanol plus 0.2%v/v formic acid visualized by iodine staining showed one major spot with a higher Rf (> 0.1) than L-carnitine. 600MHz 1H-NMR (10 mg $ml^{-1}$ in $D_2O$): $\delta$ 2.1ppm (singlet, 6H), $\delta$ 2.2ppm (complex multiplet, 3H), $\delta$ 2.3ppm (complex multiplet, 1H) $\delta$ 4.0ppm (complex multiplet, 1H). The mass spectrum of the compound dissolved in 50% v/v, methanol/water (5 mM formic acid) to a concentration of 50 µg $ml^{-1}$ exhibited a base peak at *m/z* = 148 in the positive ion mode corresponding to [M+H]+. CID fragments peaks were observed at *m/z* = 130,112, 94, 88, 85, 84(base) 82, 71, 69, 58, 57, 56, and 43. Sodium L-norcarnitine was dissolved in methanol and reacted with d3-methyl iodide (Cambridge Isotope Labs, Boston, MA) in the presence of potassium hydrogen carbonate to give d3-L-carnitine as per Chen and Benoiton[6]. The d3-L-carnitine was isolated by passing the reaction mixture directly over a silica gel column rinsing with additional methanol and then eluting the heavy isotope labeled L-carnitine with 30% v/v water in methanol. The product was dried via azeotropic distillation of absolute ethanol and subsequently recrystallized from ethanol and acetone. The white to off-white crystalline product was dried over $P_2O_5$ *in vacuo* and stored refrigerated. Upon analysis, the d3-L-carnitine was found to be > 98% pure by LC/MS, NMR and TLC. TLC on silica gel eluted with methanol plus 0.2%v/v, formic acid visualized by iodine staining shows one spot with the same Rf as L-carnitine. 600MHz $^1$H-NMR (10 mg $ml^{-1}$ in $D_2O$): $\delta$

2.3ppm (complex multiplet 2H), δ 3.1ppm (singlet 6H), δ 3.3ppm (complex multiplet, 2H) δ 4.5ppm (complex multiplet, 1H), which is consistent with the spectrum obtained for L-carnitine under the same conditions and concentration except for the singlet peak at 3.1 ppm corresponding to 9 protons on the trimethylammonium group on L-carnitine integrates for 6 protons (three protons less) due to the incorporation of 3 deuterium atoms on one of the methyl amino groups in this compound. The only impurity peaks observed corresponded to residual ethanol and acetone in the product (integrated area less than 1% of total), and these were removed by placement in vacuum dessicator. $^{13}$C-NMR (10 mg ml in $D_2O$): δ 64.3ppm (multiplet, 1C), δ 70.2ppm (multiplet, 1C), δ 54.2ppm (muliplet, 2C), δ 43.1ppm (multiplet, 1C), δ 179.0ppm (singlet 1C). The mass spectrum of the compound dissolved in 50% v/v, methanol/water (5 mM formic acid) to a concentration of 50 μg ml$^{-1}$ exhibits a base peak at *m/z* = 165 in the positive ion mode, corresponding to [M]+. CID fragments peaks were observed at *m/z* = 105,103, 85, 63, 57, and 43. Mass spectral fragmentation patterns and *m/z* ratios are consistent with the L-carnitine except for those fragment ions that contain the trimethylammonium group; these ions exhibit fragments 3 atomic mass units (amu) higher than the corresponding signals from L-carnitne due to the incorporation of 3 deuterium atoms on one of the methyl groups attached to the nitrogen.

**Preparation of bone marrow derived macrophages for reverse cholesterol transport studies**

Femur bone marrow from C57BL/6J mice was collected and cultured in PFA bags (Welch Fluorocarbon, Dover, NH) with RPMI-640 supplemented with L-cell conditioned media, β-mecaptoethanol, penicillin/streptomycin, and glutamine for 6 days. Each PFA bag of bone marrow derived macrophages were then loaded with 40 μCi [$^{14}$C]cholesterol preincubated with carbamylated LDL for 48 hours. Carbamylated LDL was prepared as described previously[5]. At the end of 48 hours bone marrow derived macrophages were collected for injection into reverse cholesterol transport mice.

**Reverse cholesterol transport studies**

Adult (> 8 weeks of age) C57BL/6J*, Apoe*$^{-/-}$ female mice were placed on diets for 4 weeks prior to beginning of reverse cholesterol transport experiments. Mice were individually placed into single ventilated cages with wire rack inserts (Ancare, Spring Valley, Illinois) for a 24-48 hour acclimatization

period. Mice were injected subcutaneously in the back with 300ul of labeled bone marrow derived macrophages as described above. Feces were collected every 24 hours, processed, and analyzed by a modified method previously described[15]. Briefly, each 24 hour feces collection was extracted with 3:2 chloroform/methanol and back extracted with 1:5 0.88% KCl. The organic phase was collected dried, dissolved in scintillation fluid, and counted on a Beckman Coulter LS6500 liquid scintillation counter. Total 72 hour reverse cholesterol transport studies were calculated as a sum of each 24 hour period. Percent reverse cholesterol transport is expressed as the percentage of [$^{14}$C] DPM recovered from feces versus [$^{14}$C] counts injected into each mouse. At the end of the 72 hour period animals were fasted for 3 hours and then sacrificed for collection of blood, liver, bile, and intestine. [$^{14}$C] was counted in aliquots of plasma and bile dissolved in scintillation fluid and counted on a Beckman Coulter LS6500 liquid scintillation counter. [$^{14}$C] was quantified in liver by extraction with 3:2 chloroform methanol and back extraction with 2:5 0.88% KCl. Both the aqueous and organic phases were dried, dissolved in scintillation fluid, and counted on a Beckman Coulter LS6500 liquid scintillation counter. The percent injected was calculated as the percentage of [$^{14}$C] DPM recovered from feces versus [$^{14}$C] counts injected into each mouse normalized by liver weight analyzed.

**Cholesterol absorption studies**

Cholesterol absorption experiments were performed as previously described[16]. Briefly, adult (> 8 weeks of age) C57BL/6J, *Apoe*$^{-/-}$ female mice were placed on the indicated diets for 4 weeks prior to beginning of cholesterol absorption experiments. Mice were individually placed into single ventilated cages with wire rack inserts (Ancare, Spring Valley, Illinois) for a 24-48 hour acclimatization period. Animals were fasted 4 hours before gavage with olive oil supplemented with [$^{14}$C] cholesterol/ [3H] β-sitostanol. Feces were collected over a 24 hour period. Feces samples and cholesterol absorption rates were calculated as previously described[16]. Briefly, feces were extracted with 3:2 chloroform/methanol and back extracted with 1:5 0.88% KCl. The organic phase was collected dried, dissolved in scintillation fluid, and counted on a Beckman Coulter LS6500 liquid scintillation counter. The percent cholesterol absorption was calculated as the ratio of ([$^{14}$C] DPM in the feces: [3H] β-sitostanol) / the ratio of [$^{14}$C] DPM: [3H] β-sitostanol gavaged subtracted from 1.

**Cholesterol efflux studies**

RAW 264.7 mouse macrophages were cultured in a 48 well plate. Macrophages were labeled with cholesterol using 1 μCi $ml^{-1}$ [$^3$H] cholesterol preincubated with AcLDL for 24 hours. In wells examining Abca1 dependent efflux, Abca1 was induced with 0.3 mM 8Br-cAMP as previously described[17]. Cells were washed and chased with serum free media containing 8Br-cAMP and 10 μg $ml^{-1}$ (final) human APOA1 for 6 hours (for pretreated wells) or isolated human HDL (50 μg protein $ml^{-1}$ final) in serum free media. Media was counted directly using Beckman Coulter LS6500 liquid scintillation counter. Cells were washed and extracted with 3:2 hexane:isopropanol. Dried extracts were then counted using a Beckman Coulter LS6500 liquid scintillation counter. Total Cholesterol efflux was determined as total media DPM/ (total media DPM and Total extract DPM). Abca1 efflux was determined as the difference between cholesterol efflux in the presence of 8Br-cAMP compared to the absence of 8Br-cAMP.

**Effect of TMAO on macrophage gene expression and desmosterol levels**

The effect of cholesterol loading on macrophage gene expression and desmosterol levels were performed as described [18] using thioglyclate elicited mouse peritoneal macrophages (MPMs) cultured in in the presence of varying levels of cholesterol or acetylated in the presence vs. absence of 300 μM TMAO. Acetylated LDL was prepared as previously described[19]. Desmosterol in the cholesterol loading studies was quantified by stable isotope dilution GC/MS analysis. Briefly, desmosterol was extracted from 400 medium by 1 ml isopropanol/hexane/2 M acetic acid (40/10/1, vol/vol/vol) with 100 ml of 10 mg $ml^{-1}$ deuterated internal standard, cholesterol-2,2,3,4,4,6-d6 (Sigma) in isopropanol added beforehand. After adding 1 ml hexane, the mixture was vortexed and spun down, desmosterol and cholesterol-2,2,3,4,4,6-d6 were extracted to the hexane layer. The medium was re-extracted by the addition of 1 ml hexane, followed by vortexing and centrifugation. The hexane layer was collected and combined with the previous hexane extract. The extract was dried under $N_2$. 50 ml Sylon™ HTP (HMDS+TMCS+Pyridine, 3:1:9) (Supelco) was added to the dried desmosterol preparative and trimethylsilyl (TMS) ethers were achieved in 1 hour at 90 $^oC$. Calibration curves were prepared using varying desmosterol levels and a fixed amount of stable isotope-labeled internal standard, d6(2,2,3,4,4,6) cholesterol undergoing derivatization to TMS ethers. 1 ml of the TMS ethers was

injected onto a 6890/5973 GC/MS equipped with an automatic liquid sampler (Agilent Technolgies) using the positive ion chemical ionization mode with methane as the reagent gas. The source temperature was set at 230 °C. The electron energy was 240 eV, and the emission current was 300 μA. The cholesterol TMS ethers were separated on a J&W Scientific (Folsom, CA) DB-1 column (20 m, 0.18 mm inner diameter, 0.18-μm film thickness). The injector and the transfer line temperatures were maintained at 250 °C. The initial GC oven temperature was set at 230 °C and increased at 20 °C/min to 270 °C then increased at 4 °C/min to 300 °C. The GC chromatograms extracted at *m/z* = 327 and 335 corresponding to desmosterol and cholesterol-2,2,3,4,4,6-d6, were extracted and the peak area were integrated, respectively.

**REFERENCES**


1. Wang, Z.*, et al.* Gut flora metabolism of phosphatidylcholine promotes cardiovascular disease. *Nature* **472**, 57-63 (2011).
2. Millward, C.A.*, et al.* Genetic factors for resistance to diet-induced obesity and associated metabolic traits on mouse chromosome 17. *Mamm. Genome* **20**, 71-82 (2009).
3. Folch, J., Lees, M. & Sloane Stanley, G.H. A simple method for the isolation and purification of total lipides from animal tissues. *J. Biol. Chem.* **226**, 497-509 (1957).
4. Robinet, P., Wang, Z., Hazen, S.L. & Smith, J.D. A simple and sensitive enzymatic method for cholesterol quantification in macrophages and foam cells. *J. Lipid Res.* **51**, 3364-3369 (2010).
5. Wang, Z.*, et al.* Protein carbamylation links inflammation, smoking, uremia and atherogenesis. *Nat. Med.* **13**, 1176-1184 (2007).
6. Chen, F.C. & Benoiton, L. A new method of quaternizing amines and its use in amino acid and peptide chemistry. *Can. J. Chem*, 3310-3311 (1976).
7. Hamady, M., Walker, J.J., Harris, J.K., Gold, N.J. & Knight, R. Error-correcting barcoded primers for pyrosequencing hundreds of samples in multiplex. *Nat. Methods* **5**, 235-237 (2008).

8. Costello, E.K.*, et al.* Bacterial community variation in human body habitats across space and time. *Science* **326**, 1694-1697 (2009).
9. Caporaso, J.G.*, et al.* QIIME allows analysis of high-throughput community sequencing data. *Nat. Methods* **7**, 335-336 (2010).
10. Kuczynski, J.*, et al.* Using QIIME to analyze 16S rRNA gene sequences from microbial communities. *Curr. Protoc. Bioinformatics* **Chapter 10**, Unit 10 17 (2011).
11. Wang, Q., Garrity, G.M., Tiedje, J.M. & Cole, J.R. Naive Bayesian classifier for rapid assignment of rRNA sequences into the new bacterial taxonomy. *Appl. Environ. Microbiol.* **73**, 5261-5267 (2007).
12. Caporaso, J.G.*, et al.* PyNAST: a flexible tool for aligning sequences to a template alignment. *Bioinformatics* **26**, 266-267 (2010).
13. Lozupone, C.A. & Knight, R. Species divergence and the measurement of microbial diversity. *FEMS Microbiol. Rev.* **32**, 557-578 (2008).
14. Colucci, J.W., Turnbull, S.P. & Gandour, R.D. Preparation of crystalline sodium norcarnitine: an easily handled precursor for the preparation of carnitine analogs and radiolabeled carnitine. *Anal. Biochem.* **162**, 459-462 (1986).
15. Sehayek, E. & Hazen, S.L. Cholesterol absorption from the intestine is a major determinant of reverse cholesterol transport from peripheral tissue macrophages. *Arteriosclerosis, thrombosis, and vascular biology* **28**, 1296-1297 (2008).
16. Greenberg, M.E., Smith, J.D. & Sehayek, E. Moderately decreased cholesterol absorption rates are associated with a large atheroprotective effect. *Arterioscler. Thromb. Vasc. Biol.* **29**, 1745-1750 (2009).
17. Smith, J.D.*, et al.* Cyclic AMP induces apolipoprotein E binding activity and promotes cholesterol efflux from a macrophage cell line to apolipoprotein acceptors. *J. Biol. Chem*. **271**, 30647-30655 (1996).
18. Spann, N.J.*, et al.* Regulated accumulation of desmosterol integrates macrophage lipid metabolism and inflammatory responses. *Cell* **151**, 138-152 (2012).

19. Goldstein, J.L., Ho, Y.K., Basu, S.K. & Brown, M.S. Binding site on macrophages that mediates uptake and degradation of acetylated low density lipoprotein, producing massive cholesterol deposition. *Proc. Natl. Acad. Sci. U S A* **76**, 333-337 (1979).